CDF/ANAL/EXOTIC/CDFR/7233
Version 1.0
8th September 2004

ID Efficiencies for Low Energy Electrons

Giulia Manca, Beate Heinemann, Martin Griffiths
University of Liverpool, Liverpool (UK)

Abstract

We present a study of the efficiencies of the identification criteria used to select electrons in the range of 8 to 20 GeV obtained selecting Drell-Yan events in Monte Carlo and data. The selection criteria have been studied and optimized for the selection of events in searches for Supersymmetry with multi-lepton signatures in the final state. All the variables used in the identification of the electrons have been analysed singularly. The choice of the isolation variable is very analysis dependent, thus the efficiency of the cut considered here will be analysed separately.

Contents

1 Introduction

The environment of hadron colliders is very challenging for the identification of electrons at low energy principally due to the high cross sections for QCD jet production, which can fake a low energy electron when a jet is really narrow in the calorimeter and has a track associated with it. We propose a preliminary set of cuts meant to identify electrons in the "medium" E_T range (between 8 and 20GeV), where the background from QCD jets is expected to be very high [1], and verify the validity in the high energy region. For this purpose we use Drell-Yan(DY) events at low invariant mass in the data and Monte Carlo; these events are expected to have two isolated, opposite sign electrons back to back in the detector and as such should be easy to identify, insuring a high purity of the initial sample. The efficiency for each of the proposed cuts is calculated individually and together with the other cuts, in two separate ways and the difference used as a systematic uncertainty. The most challenging procedure is the estimation and removal of the background, for which more studies will be necessary in the future. The efficiencies are parametrized as a function of the electromagnetic transverse energy of the probe electron (the leg on which the efficiencies are being calculated), and are cross-checked as a function of η, ϕ and of the invariant mass of the two electrons. Various checks are also performed against multiple interactions events. Special attention is given to the choice of the isolation variable and its efficiency, which is presented separately. This study is part of the studies performed in the SUSY group for identification of low energy lepton and should be considered together with the parallel efforts in the same group [2, 1].

2 Datasets (Data and Monte Carlo)

The data samples used in this studies are:

1. the 8 GeV inclusive electron dataset (dataset id: `blpc0d`). Events are selected with one electron at trigger level with the requirements listed in Table 1, and are subjected to a prescale factor of 10 for some portion of the period of data taking. The DY sample has been selected from this sample. The total luminosity of this sample is approximately 50 pb^{-1}, corresponding to data from March 2002 until February 2004.

2. the `DIELECTRON_CENTRAL_4` path of the `SUSY_DILEPTON` dataset (`edil0d`), where events are selected at trigger level with at least two electrons satisfying the selection criteria listed in Table 2 (middle column). The events are further filtered requiring at least two electrons with the requirements in Table 2, rightmost column.

The Monte Carlo samples are:

1. the Drell-Yan sample, generated with a lower cut of $M_{\ell\ell} > 5$ GeV/c^2(dataset id: `sexo7t`); this sample corresponds to 410,000 events in all lepton flavours. Only events with two electrons at generator level are selected, corresponding to one third of the all sample.

5.3.1 data and Monte Carlo are analysed using the 5.3.3 version of the CDF software, with the Stntuple package dev_242.

Variable	**Level-3 Cuts**
region	central
E_T	> 8 GeV
p_T	>8 GeV/c
Had/EM	< 0.125
Lshr	<0.2
χ^2_{strip}	<10.0
χ^2_{wire}	<15.0
ΔX	< 3.0 cm
$\|\Delta Z\|$	<5.0 cm

Table 1: *Cuts applied for the selection of electrons from the* `ELECTRON_8` *trigger at Level-3.*

Variable	**Level-3 Cuts**	**Stripping Cuts**
region	central	central
E_T	> 4 GeV	> 8 GeV
Had/EM	< 0.125	$< 0.055 + 0.0045\times E$
p_T	>4 GeV/c	>4 GeV/c
E/p		<2.0(∗)
Lshr	<0.2	<0.2
χ^2_{strip}	<20.0	<10.0
Q·ΔX		$-3.0 < Q\cdot\Delta X < 1.5$ cm
$\|\Delta Z\|$	<8.0 cm	<3.0 cm

Table 2: *Cuts applied for the selection of electrons from the* `DIELECTRON_CENTRAL_4` *trigger at Level-3(middle column) and at stripping level(rightmost column).*

3 Central Electron Identification Variables

The variables used for the identification of the electrons and the values chosen are listed in Table 3. A complete explanation of the variables and the chosen values to cut on can be found elsewhere [3, 4, 5]. Apart for the selection on the energy and momentum of the electrons, the variables are the same as in the selection of high-p_T electrons, with similar values. The value of the cut on the E/p variable has been tightened to 1.8 to help reduce the background[6]. All electrons which are found to be part of a conversion pair[1] are removed from the data.

	Variable	Tight Central Cut
kinematic cuts		
	E_T	> 8 GeV
	p_T	>4 GeV/c
	Fiduciality	fidEle = 1 (CES based)
	Z_{vertex}	$\lvert z_0^{track}\rvert <60.0$ cm
identification cuts		
	Had/EM	$< 0.055 + 0.0045\times E$
	E/p	$<1.8(*)$
	Lshr	<0.2
	χ^2_{strip}	<10.0
	Q$\cdot\Delta X$	$-3.0 < Q \cdot \Delta X < 1.5$ cm
	$\lvert\Delta Z\rvert$	<3.0 cm
	E_T^{iso}/E_T	< 0.1
opposite sign charge $\lvert\Delta\Phi_{\rm ee}\rvert > 150^o$		

Table 3: *Criteria for the selection of electron candidates used in this study. The central-central DY candidates require at least one tight electron and at least one other electron (with all the cuts applied apart for the one we are studying) with $\Delta\Phi > 150^o$.(*) The E/p cut is released for electrons with $p_T >$ 50 GeV/c.*

[1] An electron is defined as part of a conversion pair if its track and any other track in the event satisfy the following requirements: a) opposite sign; b) separation between the tracks smaller than 0.5 cm, and c)$\Delta cot(\theta)$ between the tracks < 0.1.

4 Central Electron Efficiencies

The two methods used for the calculation of the efficiencies are described in section 4.1 and 4.2. In both cases Drell-Yan candidate events are selected with one electron satisfying all the cuts in Table 3, and a second electron with a track of opposite sign charge(OS) and with $|\Delta\Phi|$ between the two tracks $> 150^o$. A plot of the invariant mass and $|\Delta\Phi|$ distribution of the opposite sign two electrons when all the identification cuts in Table 3 are applied apart from the isolation is shown in Figure 8. The number of events with two electrons with same charge track(SS) is considered a good estimate of the background and as such it is subtracted from the number of opposite sign events in the calculation of the efficiencies. The distributions are shown before and after the $|\Delta\Phi|$ requirement, after the SS background subtraction. The agreement between Monte Carlo and data with background subtraction is good; the background contribution is evident in the low invariant mass window.

4.1 Method I

4.1.1 (N-1) Efficiencies

In this method we start with a sample of events with one electron satisfying all the cuts in Table 3, and a second electron satisfying all the cuts but the one which is tested. The efficiency for cut "i" is then defined as:

$$\epsilon_i = \frac{N_{AA}}{N_{A(A-i)}}, \tag{1}$$

where

- N_{AA} is the number of events with two OS electrons passing all cuts in Table 3, subtracted by the number of same sign events, and
- $N_{A(A-i)}$ is the number of events when one electron passes all the cuts and the second electron passes all the cuts but the cut we are testing (the *i-th* cut), subtracted by the number of same sign events.

Only the first two electrons in the event are selected, and a random function is used to decide which one will be tested against "all" tight cuts and which one against "all minus one". Figures 1 and 2 show the distributions of the identification variables for the selected electrons when all the cuts but the one on the variable shown have been applied ("N-1" plots). The data appear to be well described by the Monte Carlo apart for Had/Em

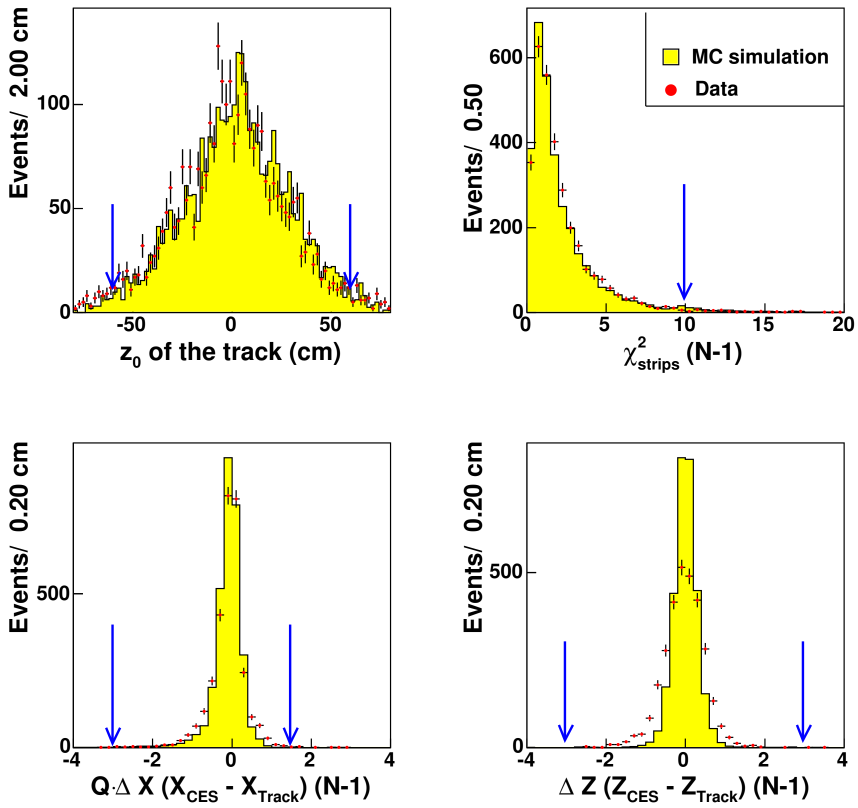

Figure 1: *The electron variables used for the selection of the Drell-Yan candidates from the 8* GeV *electron data (dots) and in the signal Monte Carlo (solid histogram). The OS electrons candidates have been selected applying all the cuts but the one whose distribution is plotted ("N-1"). The arrows indicate the value where the cut has been placed. No background subtraction is applied.*

and ΔZ. The efficiencies in this way determined have been parametrized as a function of the electromagnetic energy of the second electron in bins of 8-12,12-16,16-20,20-30,30-35,35-40,40-50,50-60, and >60 GeV. In Figure 3 and Figure 4 no isolation cut has been applied to the second leg at the denominator and numerator; in Figures 5 and 6 the cut $E_T^{iso}/E_T < 0.1$ has been applied to both. Few observations can be made:

- The data agree well with the Monte Carlo independently on the isolation cut. The largest difference of about 5% is seen for E/p.
- The efficiency of the E/p cut is very high in the first bins of energy and and then stabilizes on values similar to those observed in [4]. Such a behaviour might indicate that we are testing the trigger leg for which the tight cuts on the E_T and p_T of the

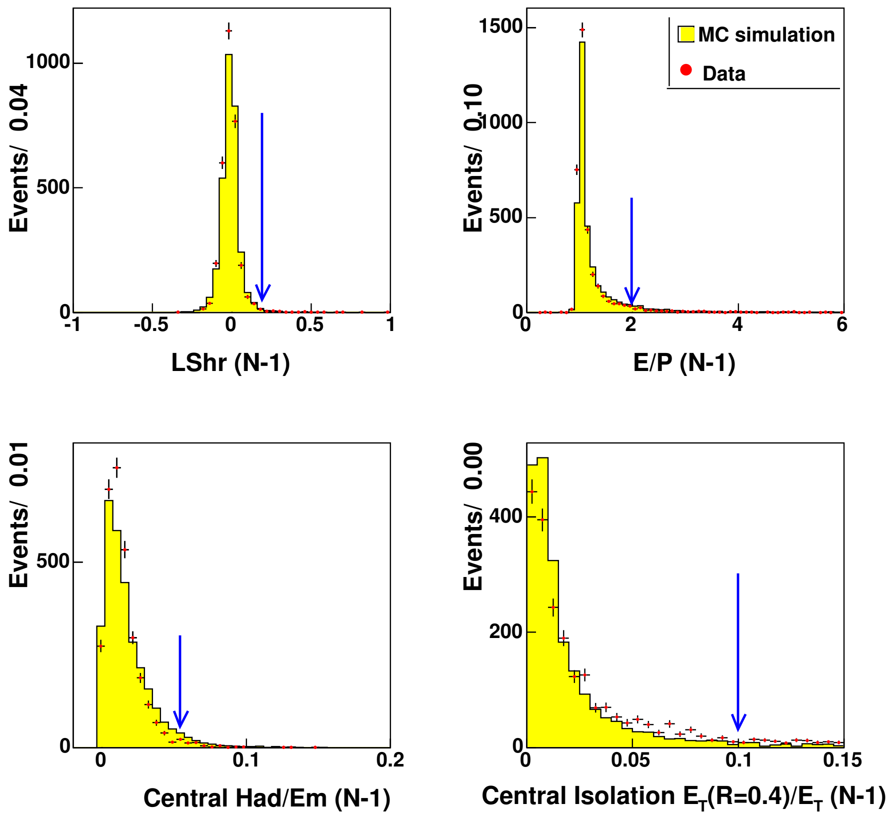

Figure 2: *The electron variables used for the selection of the Drell-Yan candidates from the 8* GeV *electron data (dots) and in the signal Monte Carlo (solid histogram). The OS electrons candidates have been selected applying all the cuts but the one whose distribution is plotted ("N-1"). The arrows indicate the value where the cut has been placed. No background subtraction is applied.*

electron would force the E/p to be effectively very close to one. To make sure that there is no trigger bias on the second leg for this variable, we have repeated the test on the data and Monte Carlo releasing the E/p requirement to $E/p < 4$. The efficiency is higher as expected, indicating the absence of bias. More studies will be necessary on this variable.

- The efficiency of the Had/EM cut in the Monte Carlo versus E_T and M_{ee} (19) has a raising trend up to $E_T\tilde{2}5$ GeV (M_{ee} 40-60 GeV/c^2), and then seems to fall again. This behaviour has still to be understood.

- In some cases the efficiency in the data is higher than in the Monte Carlo. This can be an indication of an overestimate of the background and will be studied further in the next version of this note.

The efficiencies as a function of M_{ee}, η and ϕ are shown in section A.1, A.2 and A.3. The isolation cut has been applied. No significant dependence is observed, apart from the E/p cut, which is less efficient at higher η as the electrons go through more material in the detector and thus bremsstrahlung more. Moreover, the E/p efficiency also shows some dependency on the invariant mass of the two electrons and is currently under investigation. The distributions versus ϕ are being reproduced including the correction for the track curvature [7] and will be updated in the next update of this study.

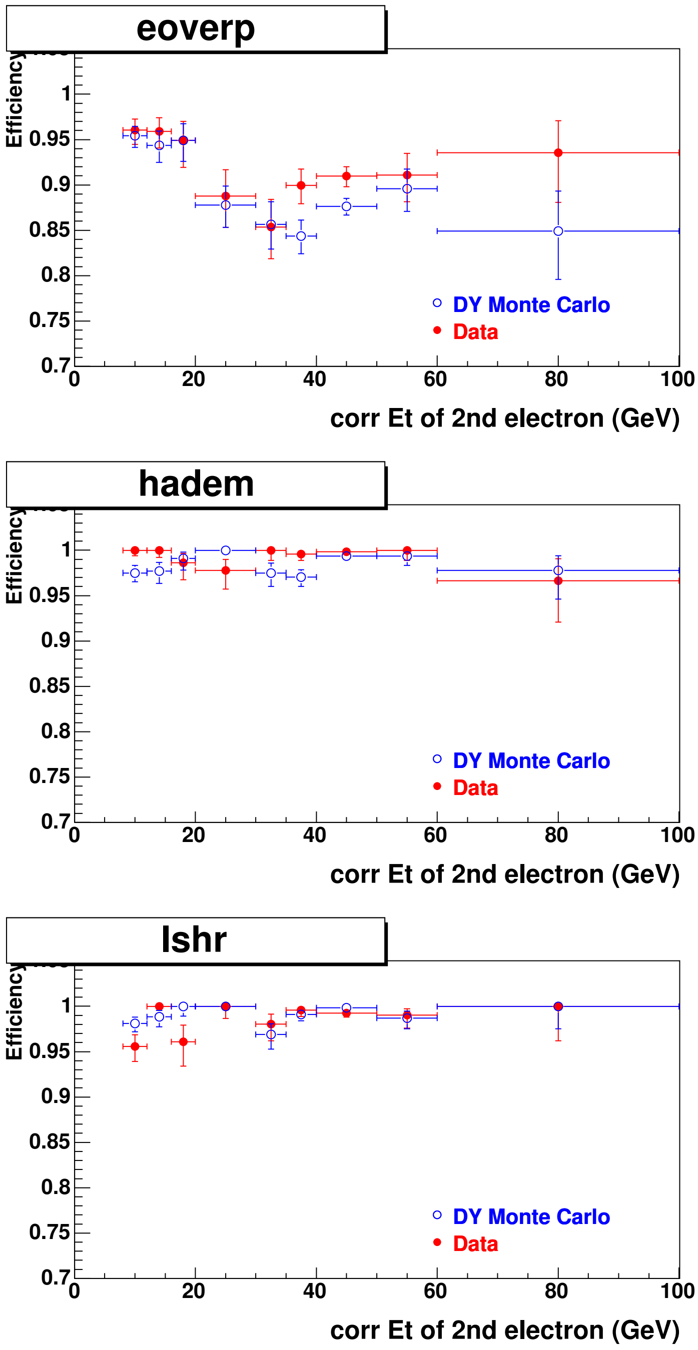

Figure 3: *The "N-1" efficiencies of the electron variables used in the selection of the electron candidates, when all the cuts but isolation and the one which is being tested are applied. All the efficiencies are plotted as a function of the electromagnetic energy of the second leg, in bins of variable size as explained in the text, for 8* GeV *electron data (filled red dots) and Monte Carlo (empty blue dots).*

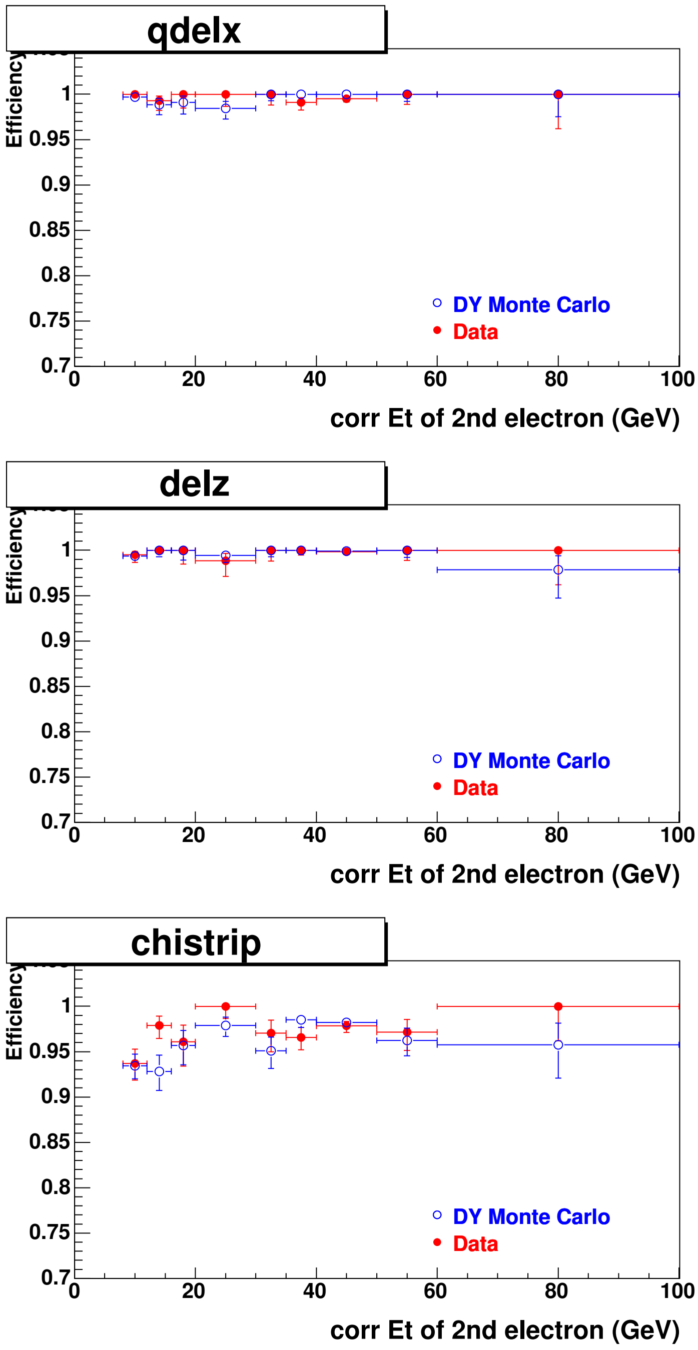

Figure 4: *The "N-1" efficiencies of the electron variables used in the selection of the electron candidates, when all the cuts but isolation and the one which is being tested are applied. All the efficiencies are plotted as a function of the electromagnetic energy of the second leg, in bins of variable size as explained in the text, for 8* GeV *electron data (filled red dots) and Monte Carlo (empty blue dots).*

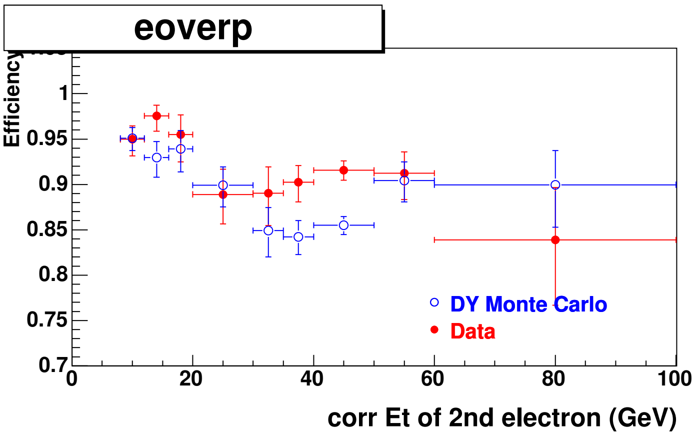

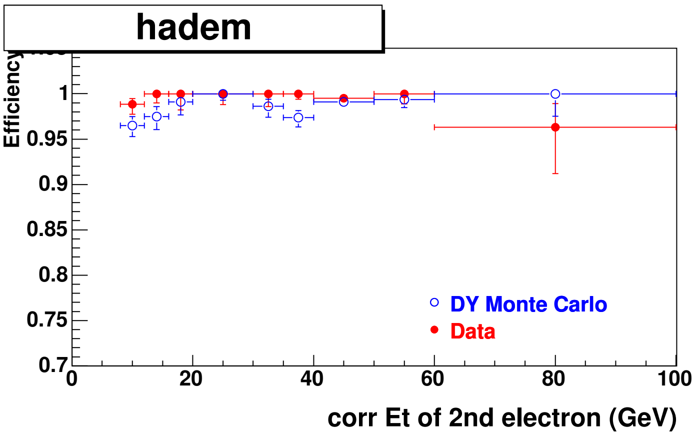

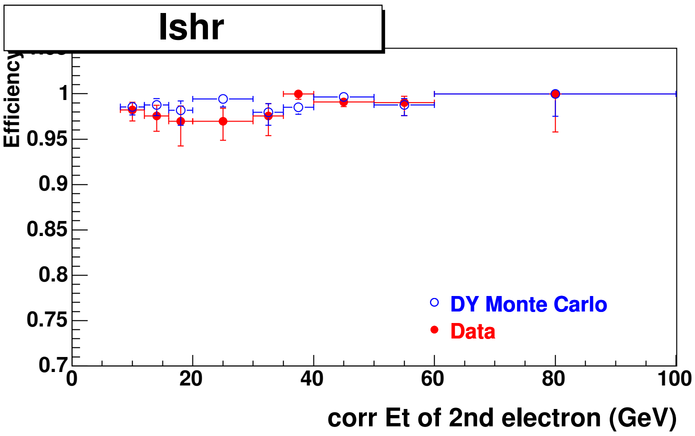

Figure 5: *The "N-1" efficiencies of the electron variables used in the selection of the electron candidates, when all the cuts but the one which is being tested are applied. Note that isolation is required. All the efficiencies are plotted as a function of the electromagnetic energy of the second leg, in bins of variable size as explained in the text, for 8* GeV *electron data (filled red dots) and Monte Carlo (empty blue dots).*

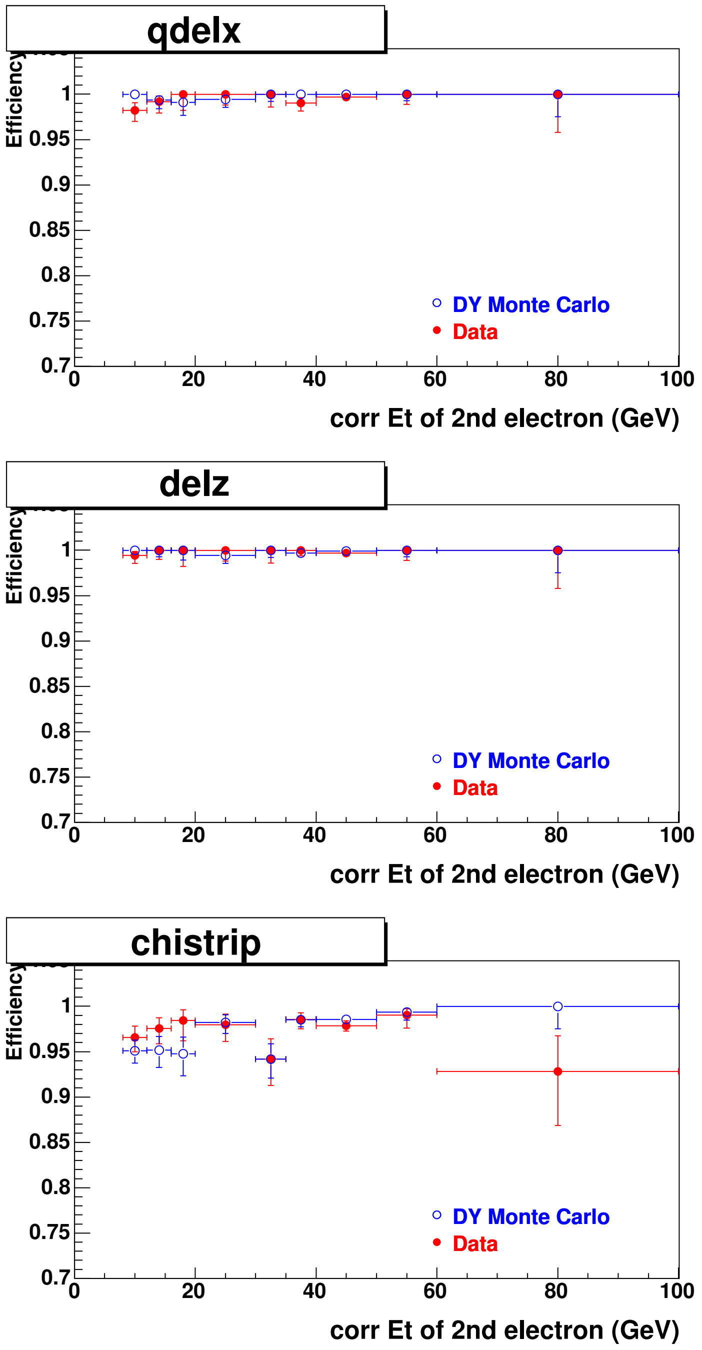

Figure 6: *The "N-1" efficiencies of the electron variables used in the selection of the electron candidates, when all the cuts but the one which is being tested are applied. Note that isolation is required. All the efficiencies are plotted as a function of the electromagnetic energy of the second leg, in bins of variable size as explained in the text, for 8* GeV *electron data (filled red dots) and Monte Carlo (empty blue dots).*

4.1.2 Isolation Efficiency

The efficiency of the isolation variable has been studied separately using the same formula in equation 1. Three variables have been considered,

- the total calorimeter isolation [2] in a cone of 0.4 around the electron E_T^{iso};
- the ratio of the latter to the EM energy of the electron (corrected for leakage);
- the track isolation, defined as the sum of the p_T's of all the tracks in a cone of 0.4 around the electron track, subtracted by the p_T of electron track itself.

The distributions of these variables are shown in Figure 7 for 8 GeV electron data and Monte Carlo. The cuts which have been studied are $E_T^{iso}/E_T < 0.1$, $E_T^{iso} < 2$ and track isolation< 0.1. The distribution of $\Delta\Phi$ of the two electrons and the invariant mass before and after the $\Delta\Phi$ cut are shown in Figure 8, where both electrons have been selected with all the cuts but the isolation cut. The effect of the $\Delta\Phi$ cut is visible in the low invariant mass region in the data. The SS background, shown in red in the plots, has been subtracted. The efficiencies for the isolation variables are shown in Figure 9. The efficiency of the calorimeter isolation variables are higher at higher energy, as expected. We chose to use the isolation ratio for the selection of the electron candidates, as its efficiency is the highest and its behaviour better understood. Since we expect the isolation efficiency in the data to be affected by multiple interaction events [8], as a cross-check we calculated the efficiency for the events with only one and only two vertices. The results are shown in Figure 10. Almost no difference is observed apart from the increase of the efficiency in the first bin of energy, which is expected to be more sensitive to the effect of multiple interactions. To consider this effect, we corrected the isolation for the number of vertices in the event using the factor [8]:

$$V_{corr} = 0.28 \cdot (N_{vertices} - 1), \tag{2}$$

which is subtracted from the isolation variable. The effect of the correction is shown in Figure 11 for the isolation ratio, where the efficiency with no correction is also shown for comparison (the latter is the same plot as in Figure 9). The correction has an effect only in the first two energy bins, and it is overall consistent with the Monte Carlo points. As further cross check, the efficiency of the cut on the isolation variables has been studied as a function of the invariant mass of the two electrons, in bins of 20 GeV/c^2, 0-20, 20-40, 40-60, 60-80, 80-100 and >100 GeV/c^2. The results are shown in Figure 12. Some dependence in the total isolation has been observed; especially the efficiency drops for invariant mass values immediately below to the Z^0 mass, expected due to bremsstrahlung. The isolation

[2] The isolation variable has been corrected for leakage in the neighbouring towers.

ratio is higher at higher invariant masses, as the increasing energy moves the cut towards higher values of the total isolation and thus cuts softer into its distribution. The efficiencies as a function of η and ϕ are shown in appendix A.2 and A.3.

To be consistent with the studies in the muon channel [9], the isolation efficiency has been calculated in the same way using the data from the `edil0d` sample (which is used in that study). The corresponding distributions can be found in section A.4. The efficiency of the total isolation cut (42) in the data is inconsistent with the Monte Carlo and the other sample and needs further investigation. No other significant discrepancy is found between the two data samples.

The isolation efficiency calculated using this method is found to be

$$\epsilon^{iso}(data) = 96.2 \pm 0.5(stat.)\%, \qquad \epsilon^{iso}(MC) = 95.8 \pm 0.4(stat.)\%,$$

which are consistent within the uncertainty.

4.1.3 Total Efficiency

The total efficiency for all the tight cuts has been determined selecting events from the DY sample with one tight electron and one second cluster with all the kinematic cuts described in Table 3 (for the denominator); the events where the second cluster survives all the tight cuts will be counted in the numerator. This efficiency is shown in Figure 13 without and with isolation. The uncertainties are only statistical. The values of the efficiencies in all E_T range (with and without the SS subtraction) are given in Table 4. For the way it has been defined, the tight electron efficiency is the most affected by the background subtraction, especially on the denominator where only the kinematic cuts are applied on the second leg. All the efficiencies in the data agree well with the Monte Carlo within the uncertainties.These values also agree with the efficiencies calculated in the Z invariant mass region for higher energy electrons [3, 4]. The total efficiency for the tight central electron identification cuts in the all E_T range is then found to be

$$\epsilon^{T}(data) = 80.8 \pm 0.9(stat.)\%, \qquad \epsilon^{T}(MC) = 78.1 \pm 0.7(stat.)\%,$$

including the isolation cut.

When the isolation cut is not applied on the second leg, the isolation is found to be

$$\epsilon^{T}_{no\,iso}(data) = 84.3 \pm 0.8(stat.)\%, \qquad \epsilon^{T}_{no\,iso}(MC) = 82.1 \pm 0.7(stat.)\%.$$

i-th Variable	data		Monte Carlo
	efficiency (ϵ^i) (SS subtracted)	**efficiency (ϵ^i) (no SS subtraction)**	**efficiency (ϵ^i) (no SS subtraction)**
$E/p < 1.8$	1504/1637=91.9 $\pm$ 0.7%	1507/1640=91.9 $\pm$ 0.7%	2485/2834=87.7 $\pm$ 0.6%
Had/EM < 0.055 + 0.0045$\times E$	1505/1511=99.6 $\pm$ 0.2%	1508/1516=99.5 $\pm$ 0.2%	2484/2521=98.5 $\pm$ 0.2%
$\|\Delta Z\|$ <3.0 cm	1504/1512=99.5 $\pm$ 0.2%	1507/1516=99.4 $\pm$ 0.2%	2485/2488=99.9 $\pm$ 0.1%
$Q * \Delta X$ >-3.0 cm, <1.5 cm	1504/1507=99.8 $\pm$ 0.1%	1507/1510=99.8 $\pm$ 0.1%	2485/2488=99.9 $\pm$ 0.1%
χ^2_{strip} <10.0	1504/1541=97.6 $\pm$ 0.4%	1507/1545=97.5 $\pm$ 0.4%	2485/2547=97.6 $\pm$ 0.3%
Lshr<0.2	1504/1524=98.7 $\pm$ 0.3%	1507/1528=98.6 $\pm$ 0.3%	2485/2508=99.1 $\pm$ 0.2%
$E_T^{iso}/E_T < 0.1$	1504/1563=96.2 $\pm$ 0.5%	1507/1595=94.5 $\pm$ 0.6%	2485/2595=95.8 $\pm$ 0.4%
$\epsilon^{\mathbf{T}}$	1504/1861=80.8 $\pm$ 0.9%	1507/2173=69.4 $\pm$ 1.0%	2485/3182=78.1 $\pm$ 0.7%
$E_T^{iso} < 2$	1445/1528=94.6 $\pm$ 0.6%	1456/1559=93.4 $\pm$ 0.6%	2393/2524=94.8 $\pm$ 0.4%
$Track^{iso} < 0.1$	1374/1470=93.5 $\pm$ 0.6%	1376/1484=92.7 $\pm$ 0.7%	2397/2500=95.9 $\pm$ 0.4%

Table 4: *N-1 Efficiency (ϵ^i) of each identification variable in the 8* GeV *electron data and total efficiency ϵ^T for the tight central identification cuts in the all E_T range, calculated using low mass Drell-Yan events in the data with SS event subtraction (first column) and without SS subtraction(middle column). The efficiencies for the Monte Carlo are reported in the last column. The SS subtraction is not applied on the Monte Carlo. The efficiencies for the total isolation and the track isolation variables are also shown although they are not included in the tight efficiency calculation.*

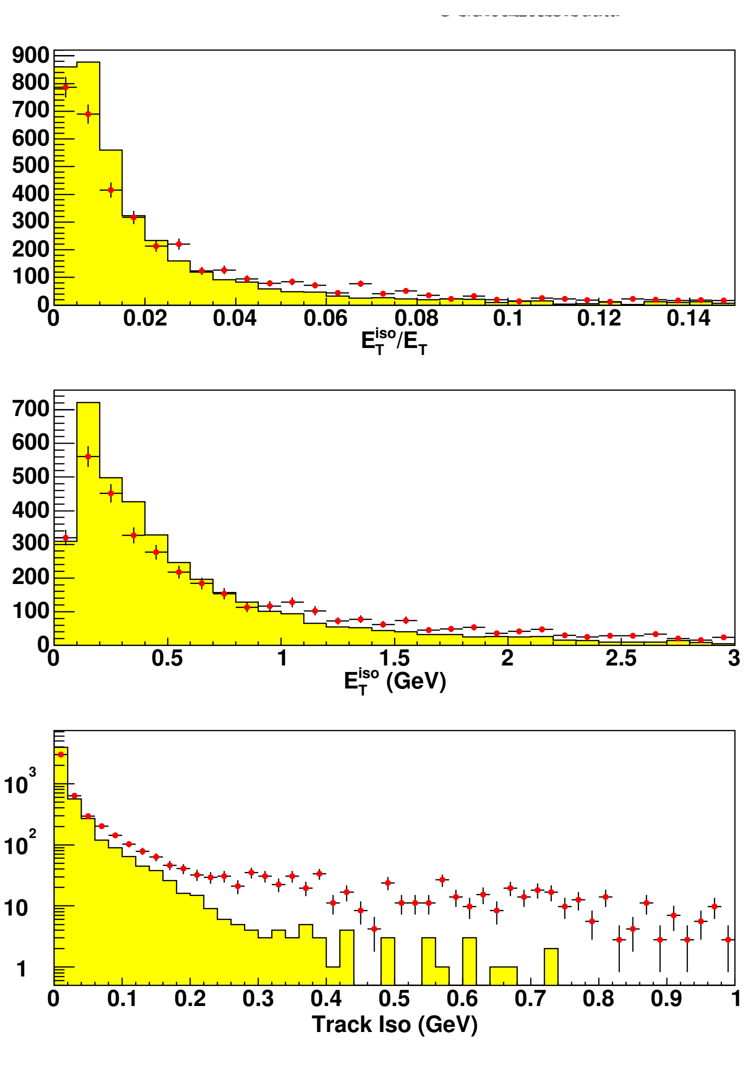

Figure 7: *The "N-1" distributions of the isolation variables:* E_T^{iso}/E_T*(top), total isolation (middle) and track isolation (bottom), for 8* GeV *electron data(dots) and Monte Carlo(solid histogram). The agreement is good for the calorimeter isolations. The shape of the track isolation in the data indicates the presence of additional background.*

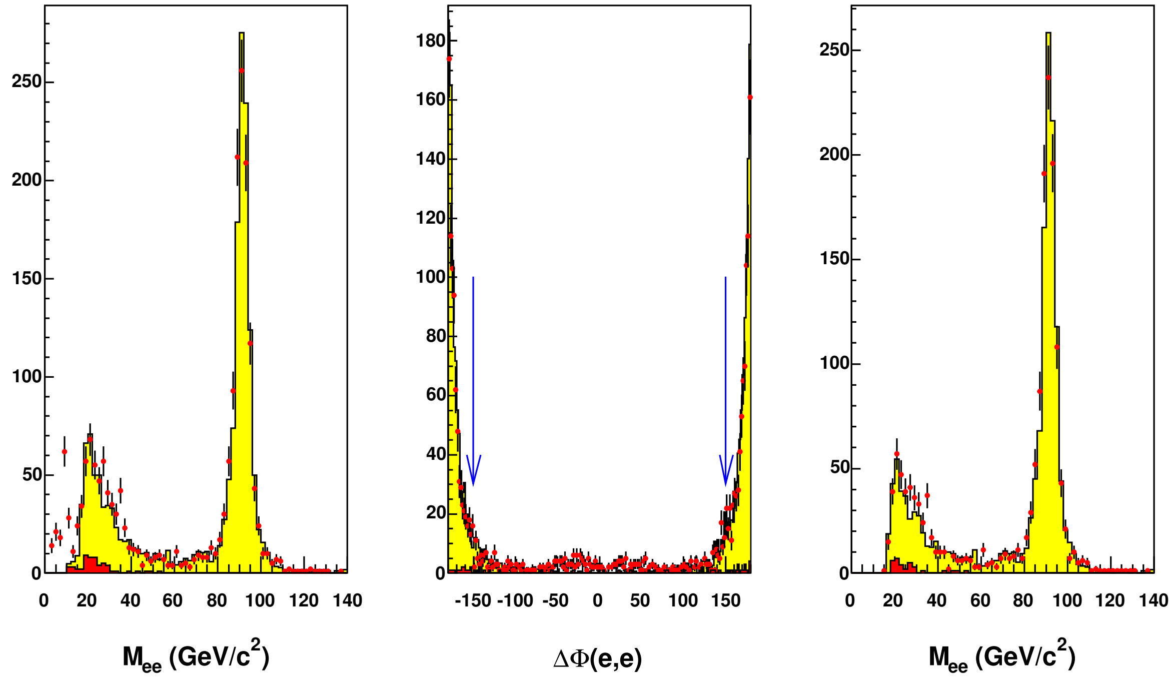

Figure 8: *The* $\Delta\Phi$ *(center) and invariant mass distributions before (right) and after (left) the* $\Delta\Phi$ *cut for the OS electrons candidates selected with all the requirements but the isolation cut. The dots are 8* GeV *electron data and the solid histogram is DY Monte Carlo. The Monte Carlo distribution has been normalized to the data in the invariant mass window of 81-101* GeV/c^2. *The arrows indicate the cut at* $|\Delta\Phi| < 150^o$. *The red histogram shows the distribution of the SS events in the data, which has been subtracted.*

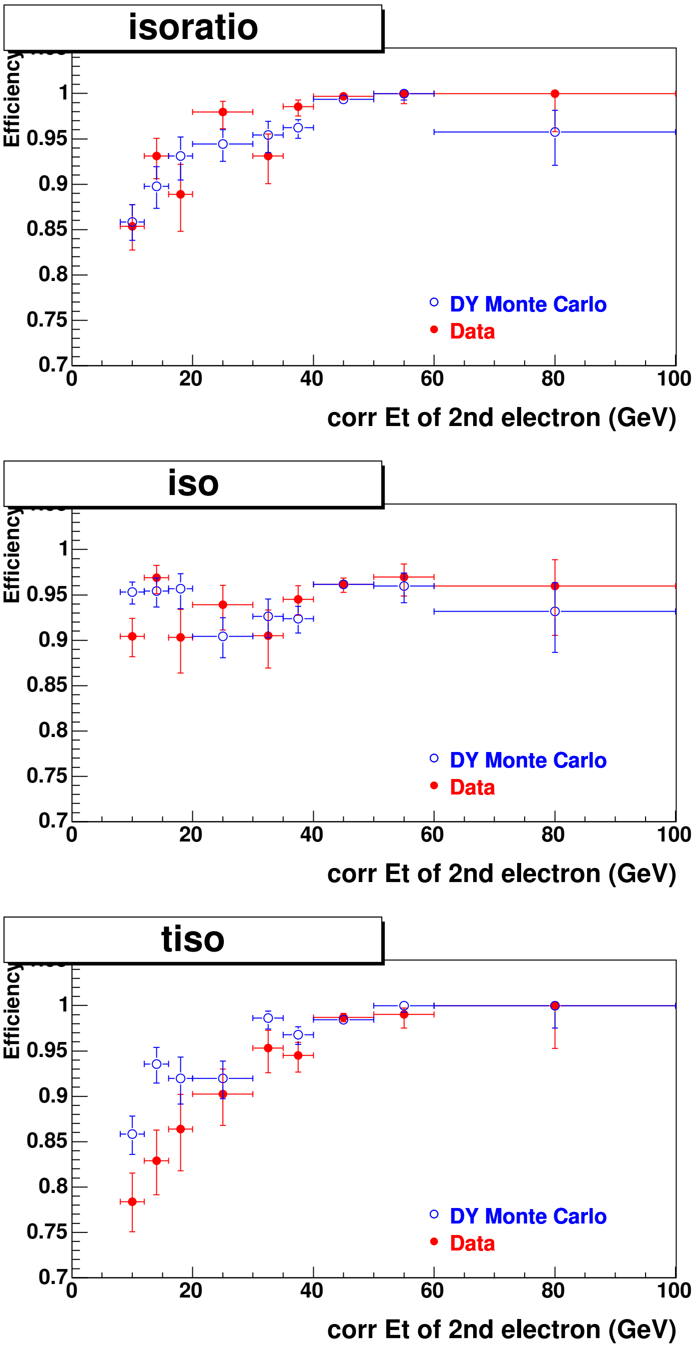

Figure 9: *The "N-1" efficiencies of the isolation variables tested in the selection of the electron candidates, when all the cuts but the isolation itself are applied. All the efficiencies are plotted as a function of the electromagnetic energy of the second leg, in bins of variable size as explained in the text, for data (filled red dots) and Monte Carlo (empty blue dots).*

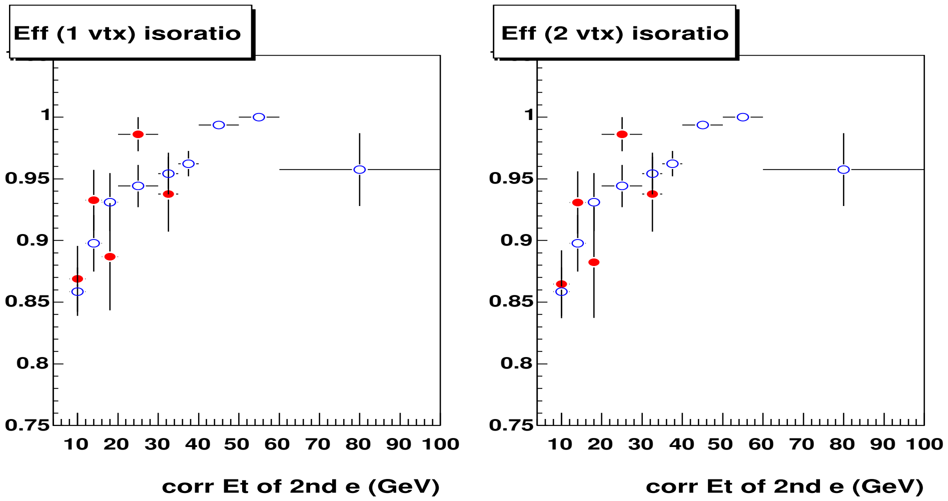

Figure 10: *The "N-1" efficiencies of the "isolation ratio" variable when all the cuts but the isolation itself are applied, in the one-vertex (left) and two-vertices(right) bin. The efficiencies are plotted as a function of the electromagnetic energy of the second leg, in bins of variable size as explained in the text, for 8* GeV *electron data (filled red dots) and DY Monte Carlo (empty blue dots).*

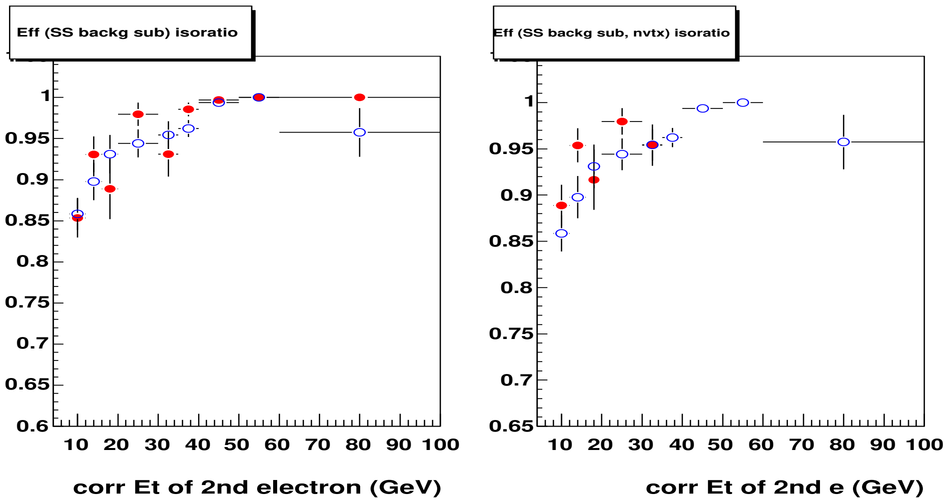

Figure 11: *The "N-1" efficiencies of the "isolation ratio" variable when all the cuts but the isolation itself are applied, with no correction(left) and when the correction for the number of vertices is applied(right). The plot on the left is the same as in Figure 9 and it is shown only for comparison. Both efficiencies are plotted as a function of the electromagnetic energy of the second leg, in bins of variable size as explained in the text, for 8* GeV *electron data (filled red dots) and DY Monte Carlo (empty blue dots).*

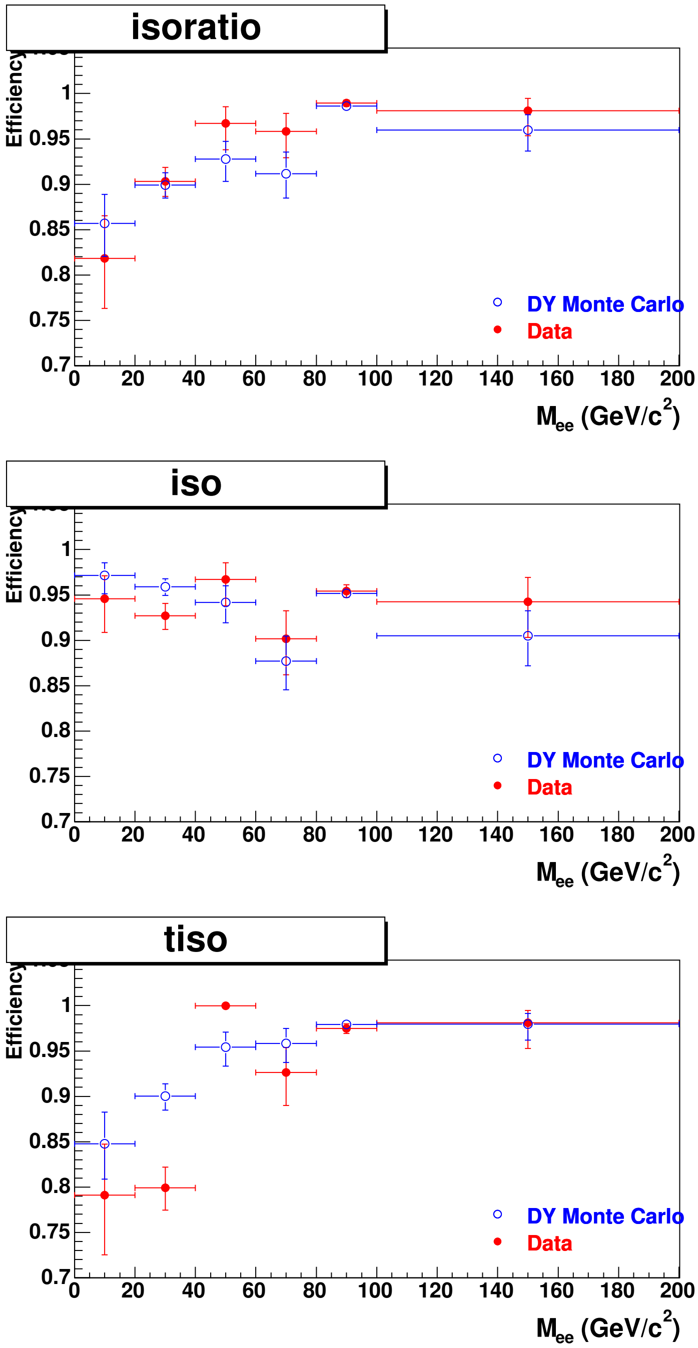

Figure 12: *The "N-1" efficiencies of the isolation variables when all the cuts but the isolation itself are applied, plotted as a function of the invariant mass of the two electrons, for 8* GeV *electron data (filled red dots) and DY Monte Carlo (empty blue dots).*

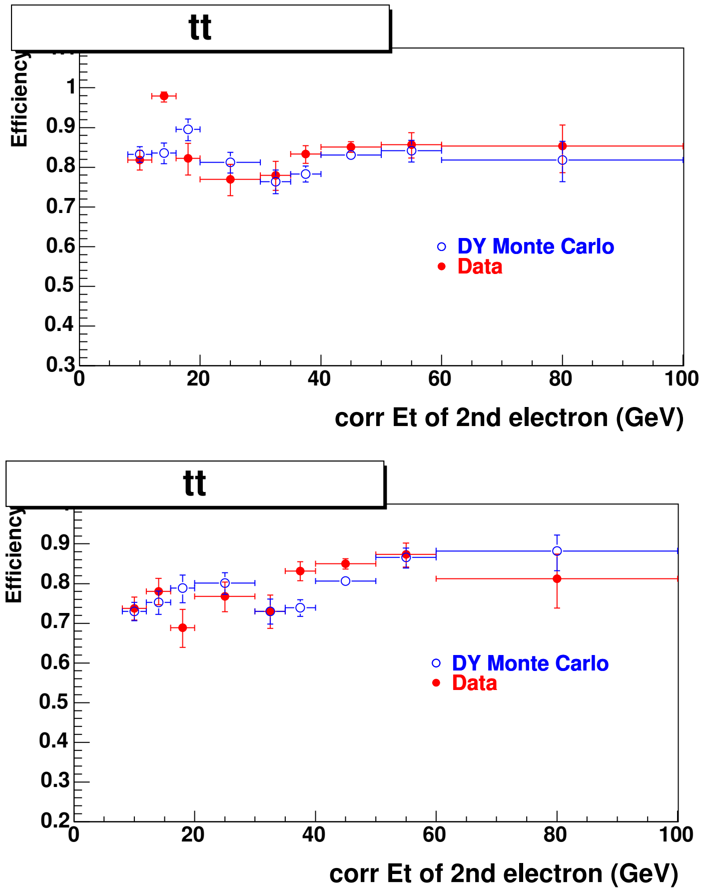

Figure 13: *The "N-1" tight efficiency of the electron variables used in the selection of the electron candidates, when all the cuts are applied. Isolation is not applied on the top plot and it is applied on the bottom plot. The efficiencies are plotted as a function of the electromagnetic energy of the second leg, in bins of variable size as explained in the text, for 8* GeV *electron data (filled red dots) and Monte Carlo (empty blue dots).*

4.2 Method II

4.2.1 ID Efficiencies

To verify the validity of method I, we have calculated the efficiencies using the method described in [3] and [8]. We start with N_{TC} = 2893 events with one tight electron and one central cluster (satisfying the kinematic requirements as in Table 3), as described in the previous section, section 3, and we apply in turn all the cuts to the second cluster, measuring the efficiency for each of them according to the expression

$$\epsilon_i \quad = \quad \frac{N_{TT} + N_{Ti}}{N_{TC} + N_{TT}}, \tag{3}$$

where N_{TT} is the total number of events with two tight electrons and N_{Ti} is the number of events satisfying the tight cuts on one leg and the *i-th* ID cut on the second leg. The number of SS events is considered a good estimate of the QCD background and as such it is subtracted from each of these numbers. When both legs pass the tight cuts, this formula becomes

$$\epsilon^T = \frac{2N_{TT}}{N_{TC} + N_{TT}} \tag{4}$$

for the tight electron efficiency. The efficiencies in this way calculated are plotted as a function of the electromagnetic transverse energy of the second electron, and are shown in Figures 14, 15, 16 and 17. The efficiencies as a function of η, M_{ee} and ϕ are plotted in appendix A.1, A.2 and A.3. The results are in very good agreement with the efficiencies obtained with the method described in section 4.1. The E/p efficiency shows the same behaviour in both cases (see also plot in Figure 21). The ΔZ cut might be related to the new version of the tracking software [6] and requires further studies. As already mentioned, the plain same sign subtraction as evaluation of the background is not valid anymore for higher energies electrons, for which the contamination of signal events (which produce same sign events as "tridents" [3]) becomes not negligible and this method gives an overestimate of the background. For the estimation of the background, we use the same method firstly used in [3] to correct the number of SS events observed in the data by subtracting the number of SS events expected from the Monte Carlo (and thus real signal). The number of OS and SS events observed in the data and the expected number of SS events after the subtraction of the MC events (scaled to the number of OS events in the data) is given in Table 5. The values of the efficiencies in the whole E_T range are given in Table 6, calculated by subtracting SS events observed in data, by subtracting the "real" QCD background (which is the number of SS events in the data corrected for the number of same sign events in the DY MC simulation), and without any SS event subtraction. We choose the "MC corrected" value as our central value. Using this method the value of the tight electron efficiency is found to be:

$$\epsilon^T(data) = 81.3 \pm 1.0(stat.)\%, \qquad \epsilon^T(MC) = 78.6 \pm 0.6(stat.)\%$$

i-th Variable	# of OS events (data)	# of SS events (data)	# of SS events (MC corrected)
N_{TC}	2893	637	625.8
$E/p < 2.0$	2320	417	411.7
Had/EM$< 0.05 + 0.0045\times E$	2479	289	283.7
$E_T^{iso}/E_T < 0.1$	2199	132	129.5
$-3.0 < Q \cdot \Delta X < 1.5$ cm	2655	435	426.5
$\lvert\Delta Z\rvert$ <3.0 cm	2694	475	468.0
χ^2_{strip} <10.0	2475	358	354.6
Lshr<0.2	2464	282	275.5
$E_T^{iso} < 2.0$	1997	52	50.3
$Track^{iso} < 0.1$	2134	114	111.0
Total (tight central electron)	1564	12	12.0

Table 5: *Number of events passing i-th variable cut for both OS and SS events in data and for the expected number of SS events after subtraction from DY Monte Carlo simulation.*

(including the isolation). As this value is in excellent agreement with the value obtained with method I, we decide to use method II as our default one, as it has already been used in other Physics groups and proved to be robust. The scale factor R from data to Monte Carlo for the total tight efficiency is

$$R^T = 1.034 \pm 0.015(stat.).$$

The value of R^T as a function of E_T is plotted in Figure 18. The value of the isolation efficiency using this method is

$$\epsilon^{iso}(data) = 94.8 \pm 0.9(stat.)\%, \qquad \epsilon^{iso}(MC) = 95.5 \pm 0.3(stat.)\%,$$

while the value of the tight efficiency without the isolation requirement (on the second leg) is found to be

$$\epsilon^T_{no\,iso}(data) = 84.5 \pm 1.0(stat.)\%, \qquad \epsilon^T_{no\,iso}(MC) = 82.4 \pm 0.5(stat.)\%$$

4.3 Systematic Studies

We estimate the systematic uncertainty using the difference between the efficiency calculated with method I and the one calculated with method II. To be conservative, we take twice this difference as an estimate of the systematic uncertainty on the efficiencies. The

i-th Variable	efficiency, ϵ^i : DATA			Monte Carlo
	(all SS sub)	(MC corr sub)	(no SS sub)	
$E/p < 1.8$	$90.7 \pm 0.7\%$	$90.6 \pm 0.7\%$	$87.1 \pm 0.5\%$	$87.2 \pm 0.4\%$
Had/EM<0.05+0.00045$\times E$	$98.3 \pm 0.7\%$	$98.1 \pm 0.7\%$	$90.7 \pm 0.5\%$	$98.2 \pm 0.2\%$
-3.0< $Q * \Delta X$ <1.5 cm	$99.1 \pm 0.5\%$	$99.0 \pm 0.5\%$	$94.7 \pm 0.3\%$	$98.2 \pm 0.2\%$
$\lvert\Delta Z\rvert$ <3.0 cm	$99.0 \pm 0.5\%$	$98.9 \pm 0.5\%$	$95.5 \pm 0.3\%$	$99.6 \pm 0.1\%$
χ^2_{strip} <10.0	$96.3 \pm 0.7\%$	$96.2 \pm 0.7\%$	$90.6 \pm 0.5\%$	$96.8 \pm 0.2\%$
Lshr<0.2	$98.1 \pm 0.7\%$	$97.9 \pm 0.7\%$	$90.4 \pm 0.5\%$	$98.8 \pm 0.1\%$
$E_T^{iso}/E_T < 0.1$	$95.0 \pm 0.9\%$	$94.8 \pm 0.9\%$	$84.4 \pm 0.6\%$	$95.5 \pm 0.3\%$
$\boldsymbol{\epsilon_T}$	$\mathbf{81.5 \pm 1.0\%}$	$\mathbf{81.3 \pm 1.0\%}$	$\mathbf{70.2 \pm 0.8}$	$\mathbf{78.6 \pm 0.6}$ %
$E_T^{iso} < 2.0$	$91.8 \pm 0.9\%$	$91.6 \pm 0.9\%$	$79.9 \pm 0.7\%$	$94.6 \pm 0.3\%$
$Track^{iso} < 0.1$	$93.8 \pm 0.9\%$	$93.6 \pm 0.9\%$	$83.0 \pm 0.6\%$	$95.0 \pm 0.3\%$

Table 6: *Efficiency (ϵ^i) of each identification variable and total efficiency ϵ_T for the tight identification cuts using DY events with SS event subtraction, QCD background subtraction, and no QCD background subtraction in data and Monte Carlo DY simulation.*

total efficiency for the tight central electron identification cuts in the all E_T range is then found to be

$$\epsilon^T(data) = 81.3 \pm 1.0(stat.) \pm 1.0(syst.)\% = (81.3 \pm 1.0)\%,$$

including the isolation cut.
The corresponding scale factor is

$$R^T = 1.034 \pm 0.015(stat.) \pm 0.018(syst.) = 1.03 \pm 0.02.$$

The value of the isolation efficiency and the scale factor are:

$$\epsilon^{iso}(data) = 94.8 \pm 0.9(stat.) \pm 2.8(syst.)\% = (94.8 \pm 2.9)\%,$$

$$R^{iso} = 0.993 \pm 0.010(stat.) \pm 0.030(syst.) = 0.99 \pm 0.03.$$

while the value of the tight efficiency without the isolation requirement and the scale factor are found to be:

$$\epsilon^T_{no\,iso}(data) = 84.5 \pm 1.0(stat.) \pm 0.4(syst.)\% = (84.5 \pm 1.1)\%,$$

$$R^T_{no\,iso} = 1.025 \pm 0.014(stat.) \pm 0.090(syst.) = 1.03 \pm 0.02.$$

4.4 Conclusions

We have calculated the efficiencies in data and Monte Carlo using two methods and found consistent results. We take one method for the central value and use twice the difference between the two as an estimate of the systematic uncertainty associated with this measurement. From these values we have extracted the scale factors data to Monte Carlo.

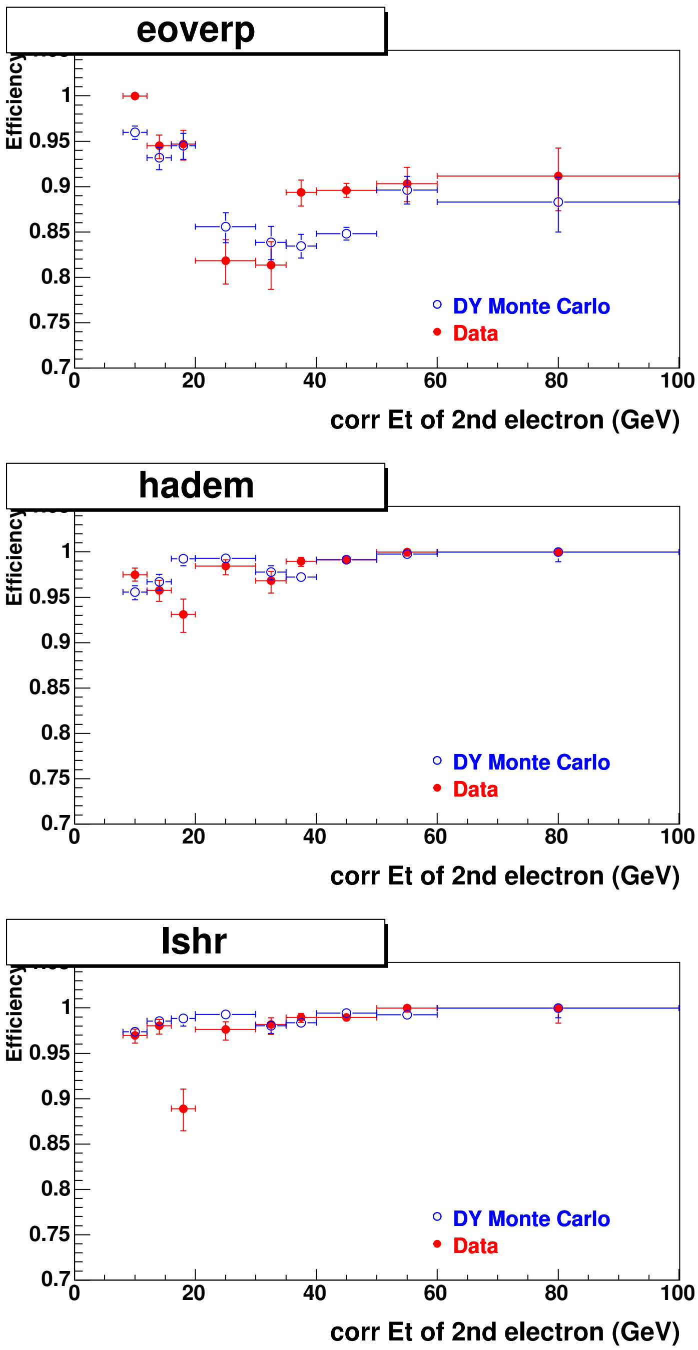

Figure 14: *The ID efficiencies of the electron variables used in the selection of the electron candidates, estimated from equation 3 as explained in the text. The efficiencies are plotted as a function of the electromagnetic energy of the second leg, in bins of variable size as explained in the text, for data (filled red dots) and DY Monte Carlo (empty blue dots).*

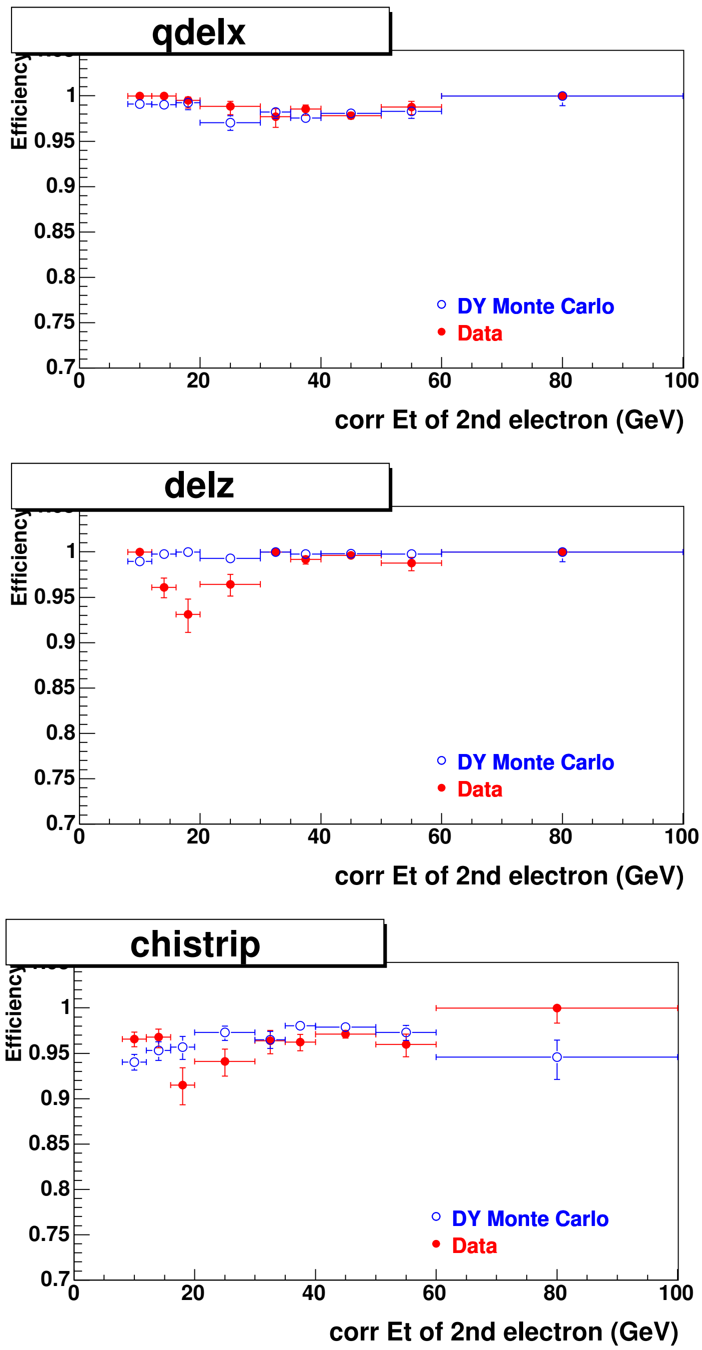

Figure 15: *The ID efficiencies of the electron variables used in the selection of the electron candidates, estimated from equation 3 as explained in the text. The efficiencies are plotted as a function of the electromagnetic energy of the second leg, in bins of variable size as explained in the text, for data (filled red dots) and DY Monte Carlo (empty blue dots).*

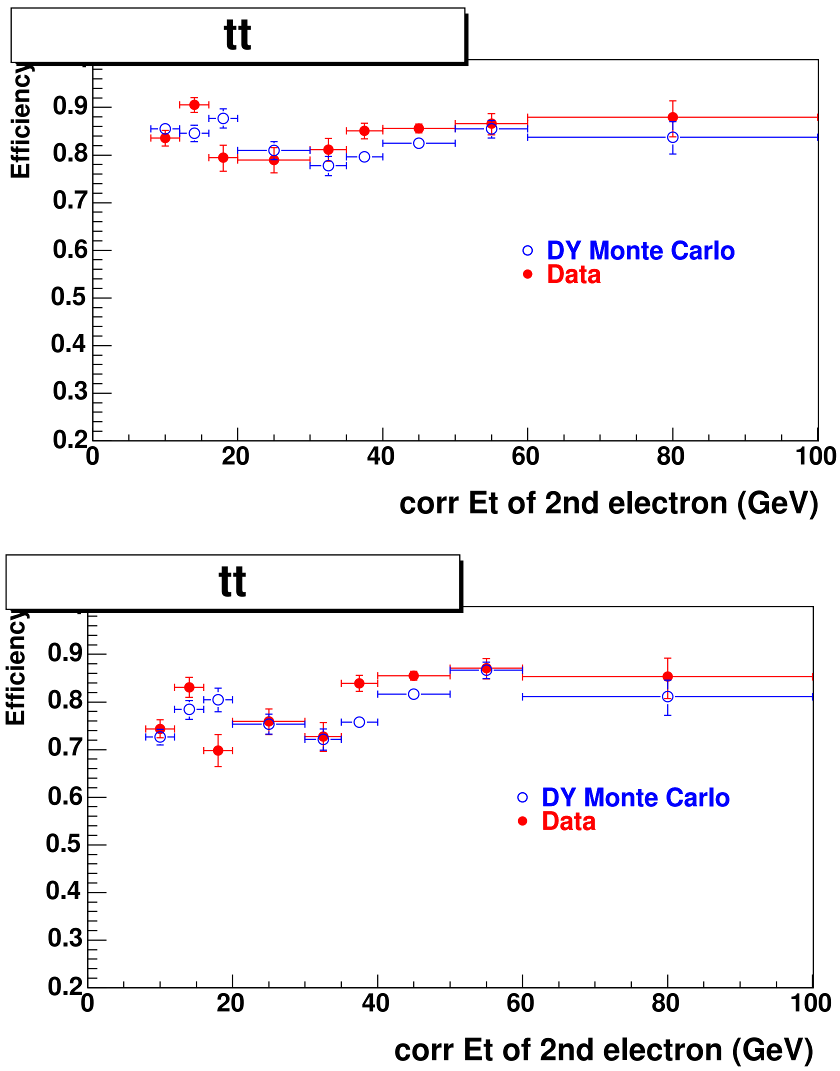

Figure 16: *The tight ID efficiency of the electron variables used in the selection of the electron candidates, without the isolation requirement (top) and when all the cuts are applied (bottom), estimated from equation 4 as explained in the text. The efficiency is plotted as a function of the electromagnetic energy of the second leg, in bins of variable size as explained in the text, for data (filled red dots) and DY Monte Carlo (empty blue dots).*

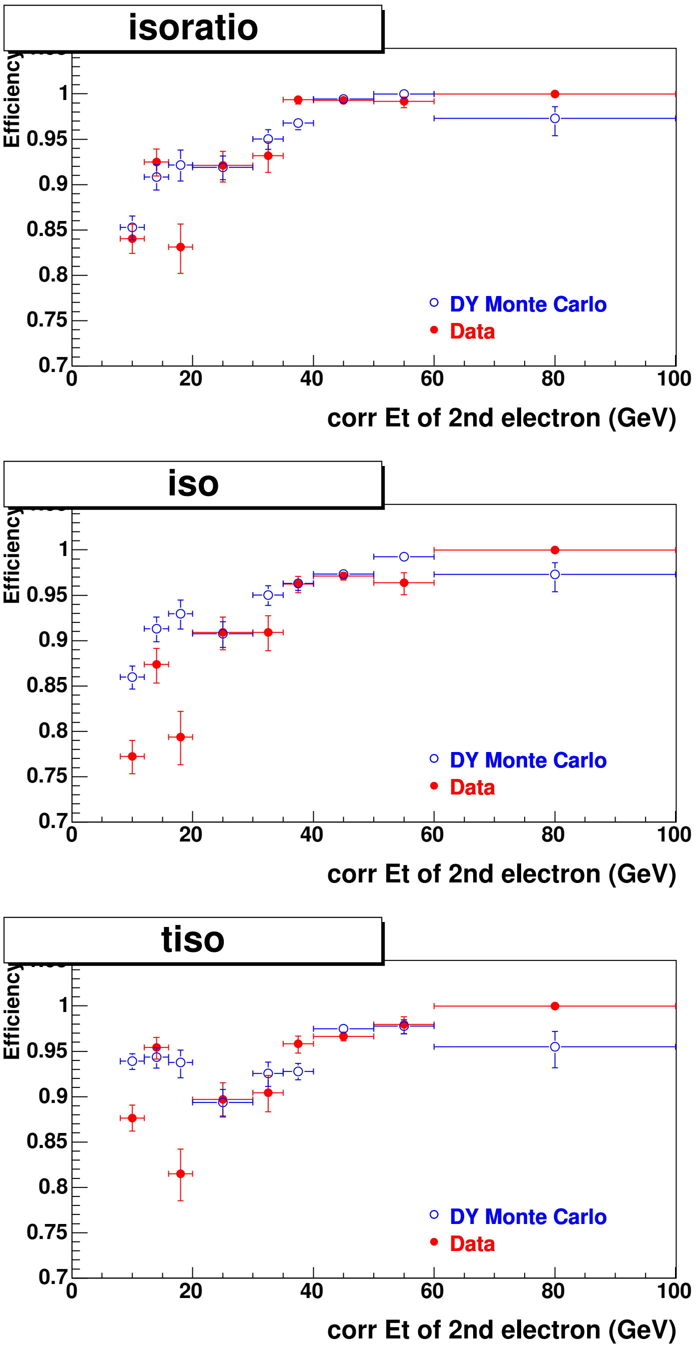

Figure 17: *The ID efficiencies of the isolation variables used in the selection of the electron candidates, estimated from equation 3 as explained in the text. The efficiencies are plotted as a function of the electromagnetic energy of the second leg, in bins of variable size as explained in the text, for data (filled red dots) and DY Monte Carlo (empty blue dots).*

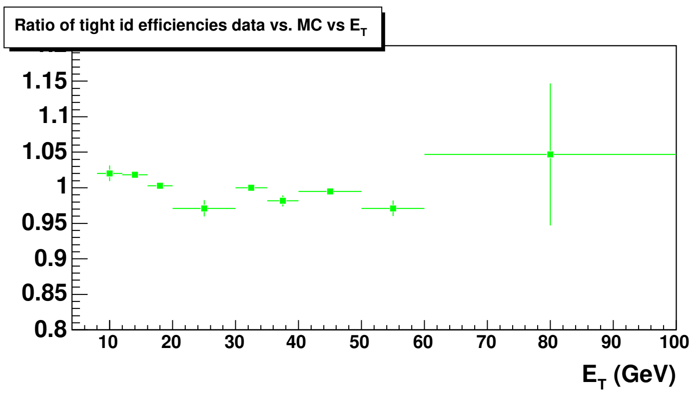

Figure 18: *The ratio of the tight ID efficiencies in data (filled red dots) and DY Monte Carlo (empty blue dots).*

5 Conclusions

We have calculated the efficiencies in data and Monte Carlo using two methods and found consistent results. We have tested the efficiencies as a function of different variables and not observed significant discrepancies. From these values we have extracted the scale factors data to Monte Carlo to be used in exotic analyses. In the future we plan to extend this study using different data sample as the $J/\Psi, \Upsilon$ and conversion samples. We also plan to improve the evaluation of the background using different methods and compare the results with the ones observed here.

6 Acknowledgments

We would like to thank Larry Nodulman and Greg Veramendi for useful discussions and suggestions. Thanks to John Zhou and Vladimir Rekovic and Michael Gold for providing the Monte Carlo and the SUSY_DILEPTON samples.

References

[1] M. Griffiths, B. Heinemann, and G. Manca, *Lepton Fake Rate in the Jet Energy Sample*. CDF Note in preparation.

[2] D. Bortoletto, E. Lytken, O. Lopez-Gonzales, and A. Canepa, *ID efficiency for intermediate pT muons*. CDF Note 7197.

[3] Giulia Manca and Young-Kee Kim, *Z^0 to electrons Cross Section measurement with Run II data*. CDF Note 6281.

[4] M. Coca, E. Halkiadakis, and S. Lockwitz, *Central Electron Identification Efficiencies for the 200 pb^{-1} Run 2 Dataset*. CDF Note 6580.

[5] ETF group, *Baseline Analysis Cuts for Central High-p_T Isolated Electrons*, June 2003. CDF Note 6454.

[6] Larry Nodulman. *Private Communication.*

[7] L. Nodulman and C. Hays, *Talks at the Joint Physics Meeting, 20 August 2004*.

[8] D. Benjamin, A. Goshaw, M. Kirby, B. Heinemann, H. Hayward, and N. Tanimoto, *Underlying Event Studies and Photon ID Efficiencies in Run II*. CDF Note 6608.

[9] Vladimir Rekovic and Michael Gold, *Isolation Efficiency for Muons.* http://fcdfwww.fnal.gov/internal/WebTalks/Archive/0406/040607_susy_lepton/06_040607_susy_lepton__other_1_5_rekovic_isoReport.pdf.

A Cross checks

A.1 Efficiencies as a function of M_{ee}

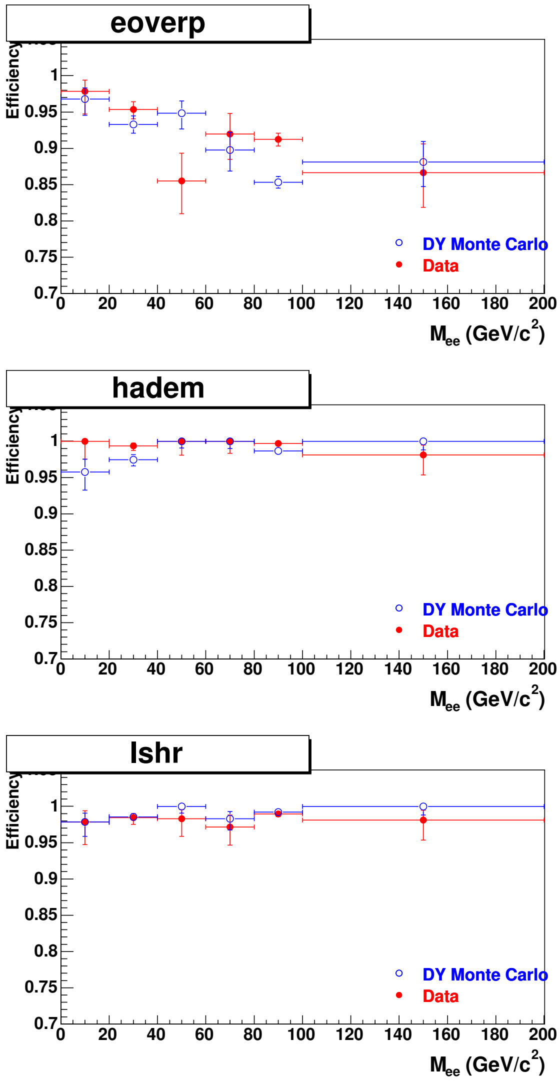

Figure 19: *The "N-1" efficiencies of the electron variables used in the selection of the electron candidates, when all the cuts but the one which is being tested are applied. All the efficiencies are plotted as a function of the invariant mass of the two electrons in bins of 20* GeV/c^2 *as explained in the text, for 8* GeV *electron data (filled red dots) and DY Monte Carlo (empty blue dots).*

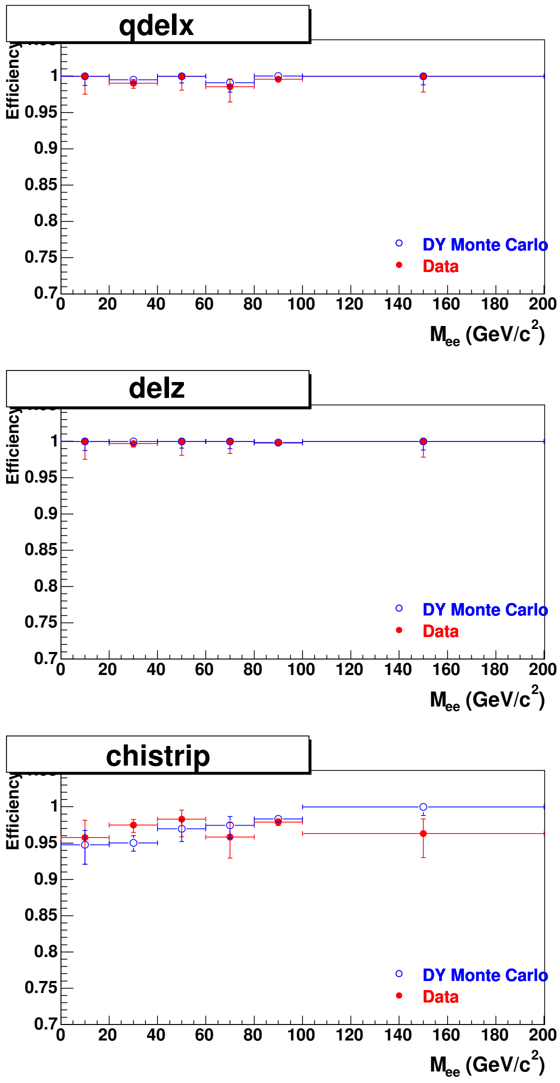

Figure 20: *The "N-1" efficiencies of the electron variables used in the selection of the electron candidates, when all the cuts but the one which is being tested are applied. All the efficiencies are plotted as a function of the invariant mass of the two electrons in bins of 20* GeV/c^2 *as explained in the text, for 8* GeV *electron data (filled red dots) and DY Monte Carlo (empty blue dots).*

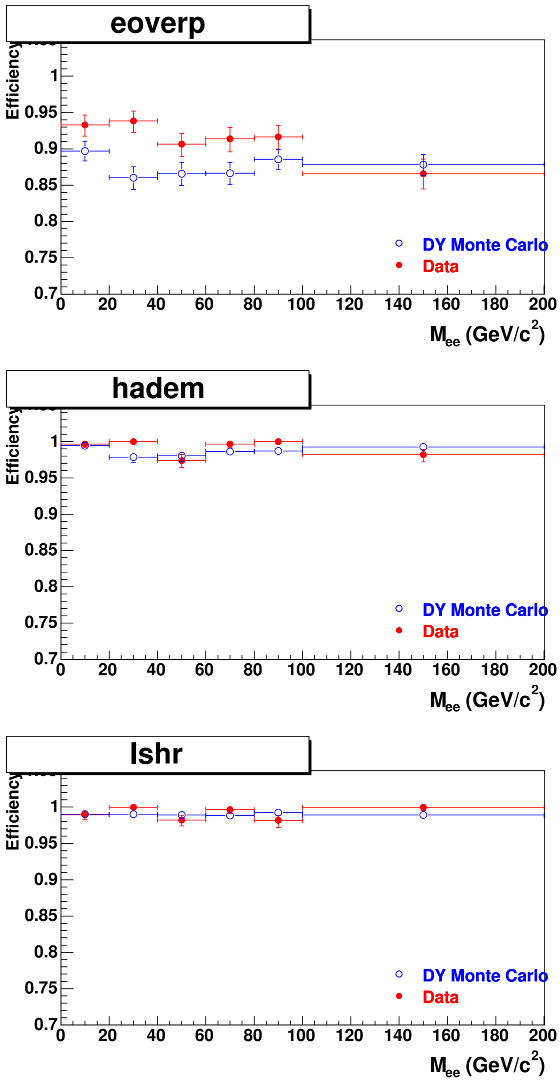

Figure 21: *The "ID" efficiencies of the electron variables used in the selection of the electron candidates, when all the cuts but the one which is being tested are applied. All the efficiencies are plotted as a function of the invariant mass of the two electrons in bins of 20* GeV/c^2 *as explained in the text, for 8* GeV *electron data (filled red dots) and DY Monte Carlo (empty blue dots).*

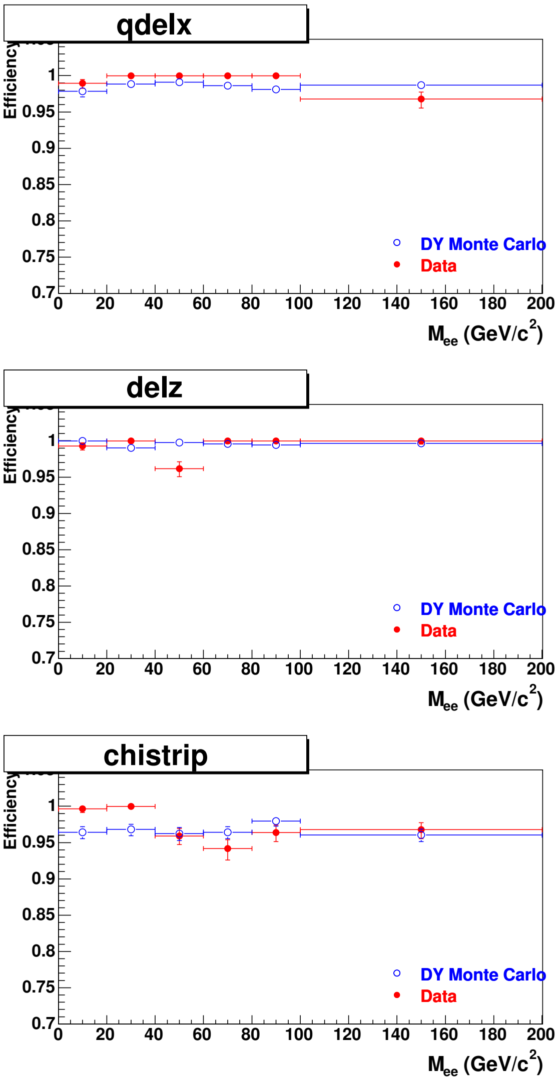

Figure 22: *The "ID" efficiencies of the electron variables used in the selection of the electron candidates, when all the cuts but the one which is being tested are applied. All the efficiencies are plotted as a function of the invariant mass of the two electrons in bins of 20* GeV/c^2 *as explained in the text, for 8* GeV *electron data (filled red dots) and DY Monte Carlo (empty blue dots).*

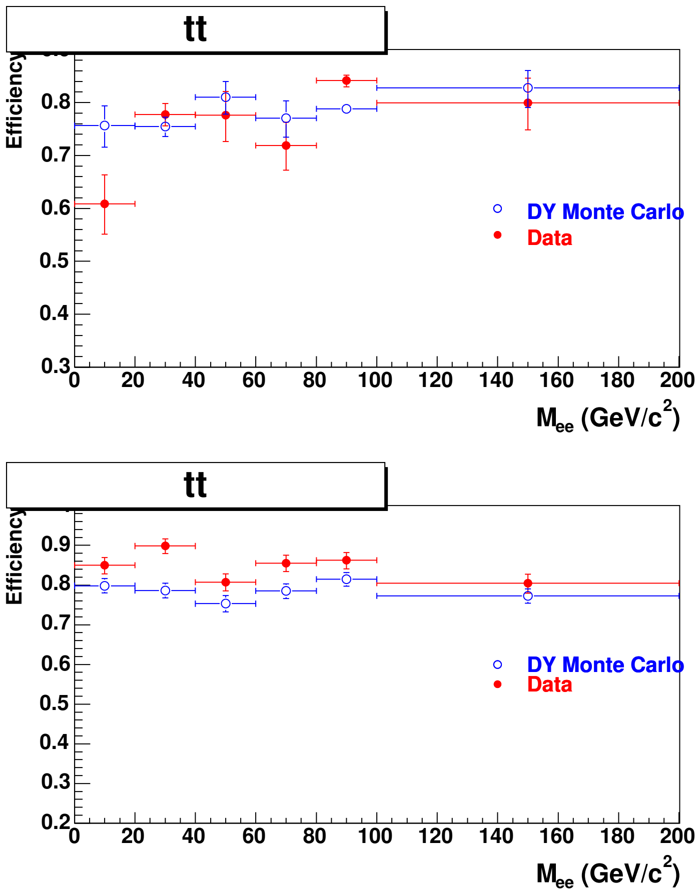

Figure 23: *The "N-1"(top) and ID(bottom) tight efficiencies of the electron variables used in the selection of the electron candidates, when all the cuts are applied. The efficiencies are plotted as a function of the invariant mass of the two electrons in bins of 20* GeV/c^2 *as explained in the text, for 8* GeV *electron data (filled red dots) and DY Monte Carlo (empty blue dots).*

A.2 Efficiencies as a function of η

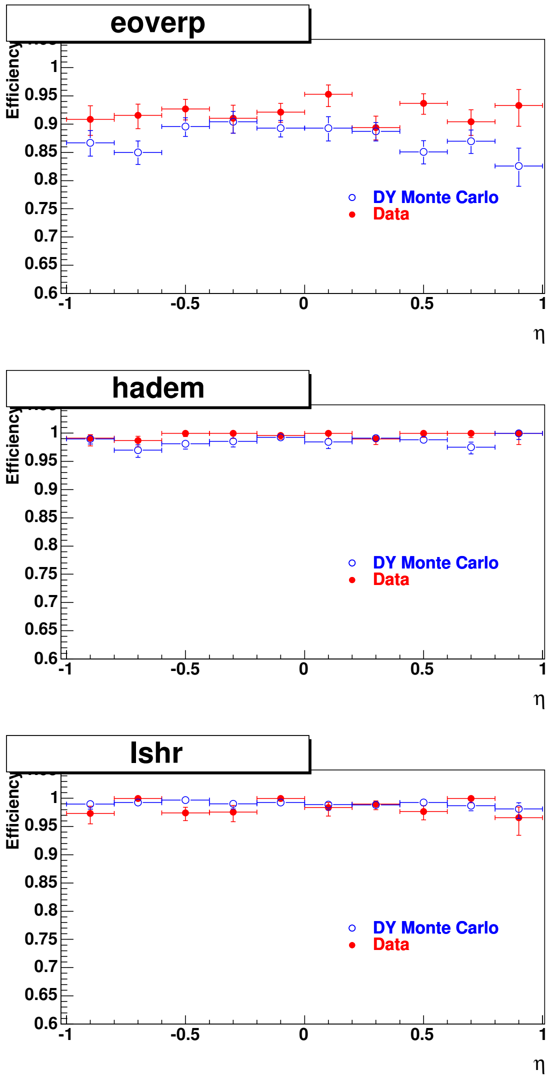

Figure 24: *The "N-1" efficiencies of the electron variables used in the selection of the electron candidates, when all the cuts but the one which is being tested are applied. All the efficiencies are plotted as a function of η of the second leg, in bins of 0.1, for 8* GeV *electron data (filled red dots) and DY Monte Carlo (empty blue dots).*

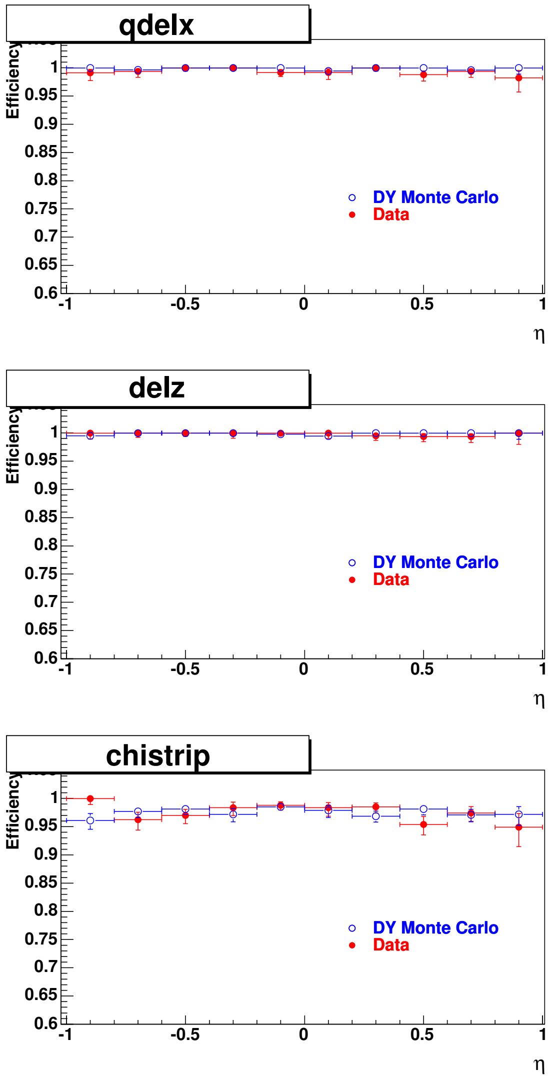

Figure 25: *The "N-1" efficiencies of the electron variables used in the selection of the electron candidates, when all the cuts but the one which is being tested are applied. All the efficiencies are plotted as a function of η of the second leg, in bins of 0.1, for 8* GeV *electron data (filled red dots) and DY Monte Carlo (empty blue dots).*

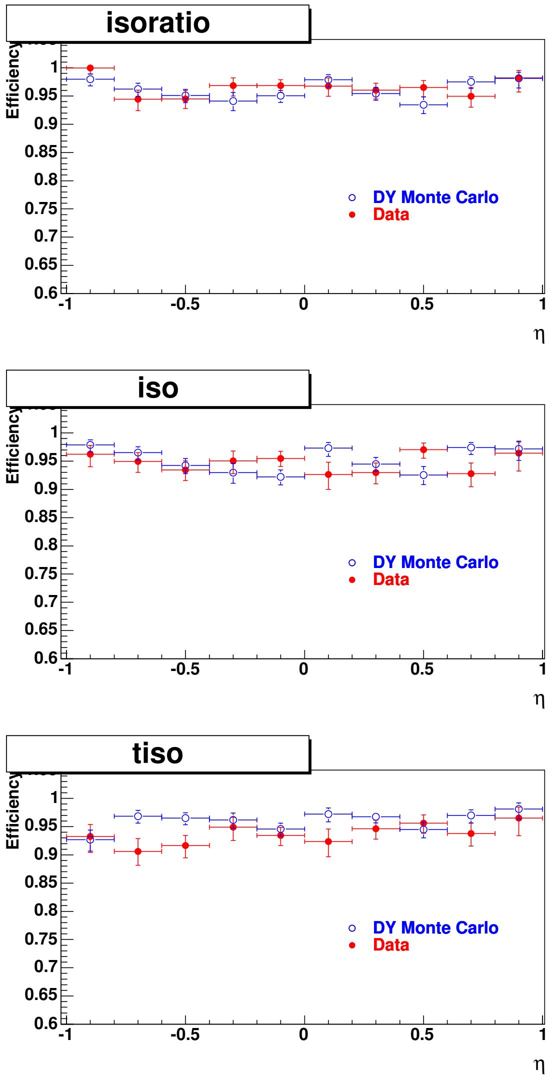

Figure 26: *The "N-1" efficiencies of the isolation variables tested in the selection of the electron candidates, when all the cuts but the isolation itself are applied. All the efficiencies are plotted as a function of η of the second leg, in bins of 0.1, for 8* GeV *electron data (filled red dots) and DY Monte Carlo (empty blue dots).*

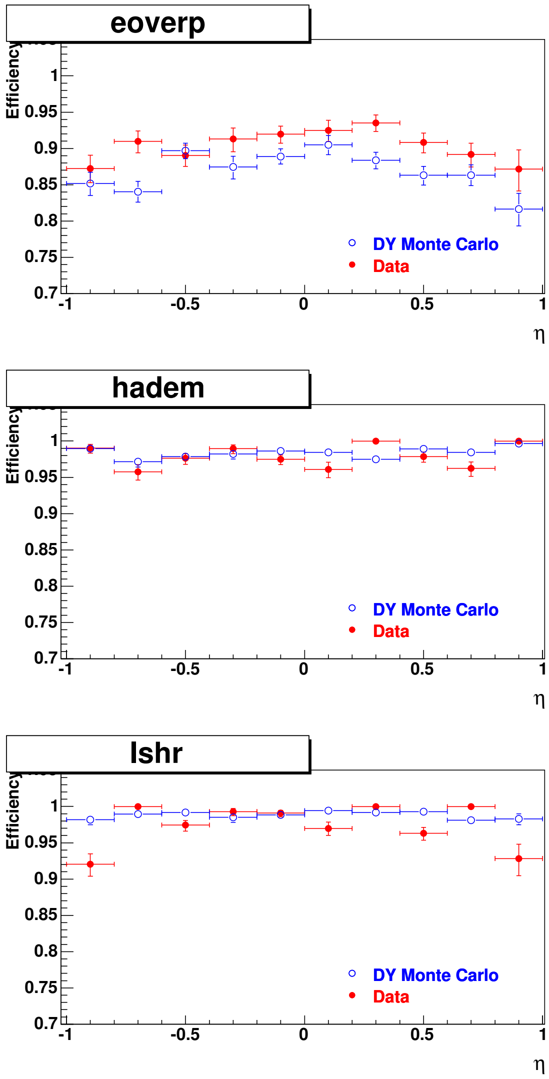

Figure 27: *The "ID" efficiencies of the electron variables used in the selection of the electron candidates, when all the cuts but the one which is being tested are applied. All the efficiencies are plotted as a function of η of the second leg, in bins of 0.1, for 8* GeV *electron data (filled red dots) and DY Monte Carlo (empty blue dots).*

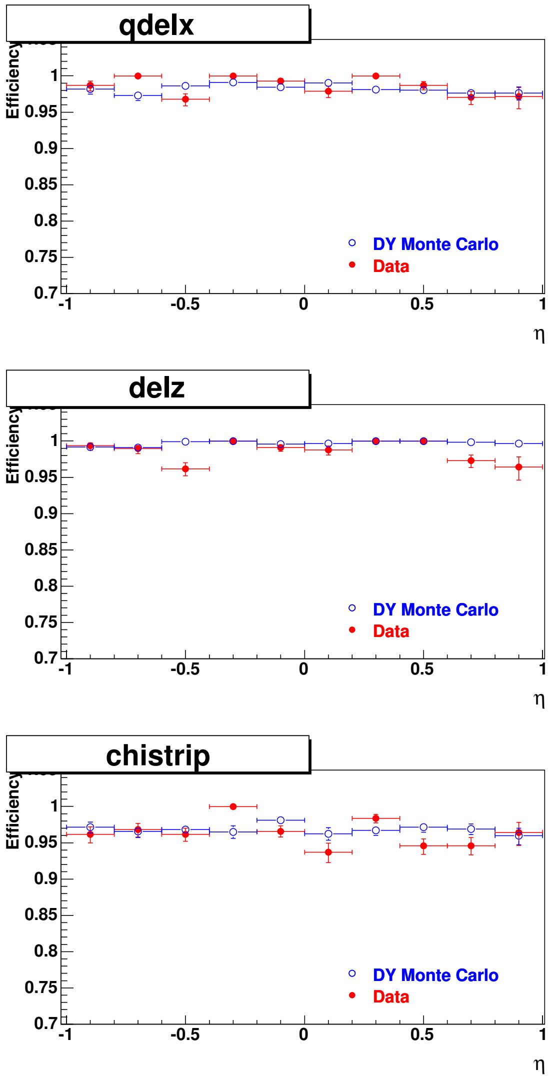

Figure 28: *The "ID" efficiencies of the electron variables used in the selection of the electron candidates, when all the cuts but the one which is being tested are applied. All the efficiencies are plotted as a function of η of the second leg, in bins of 0.1, for 8* GeV *electron data (filled red dots) and DY Monte Carlo (empty blue dots).*

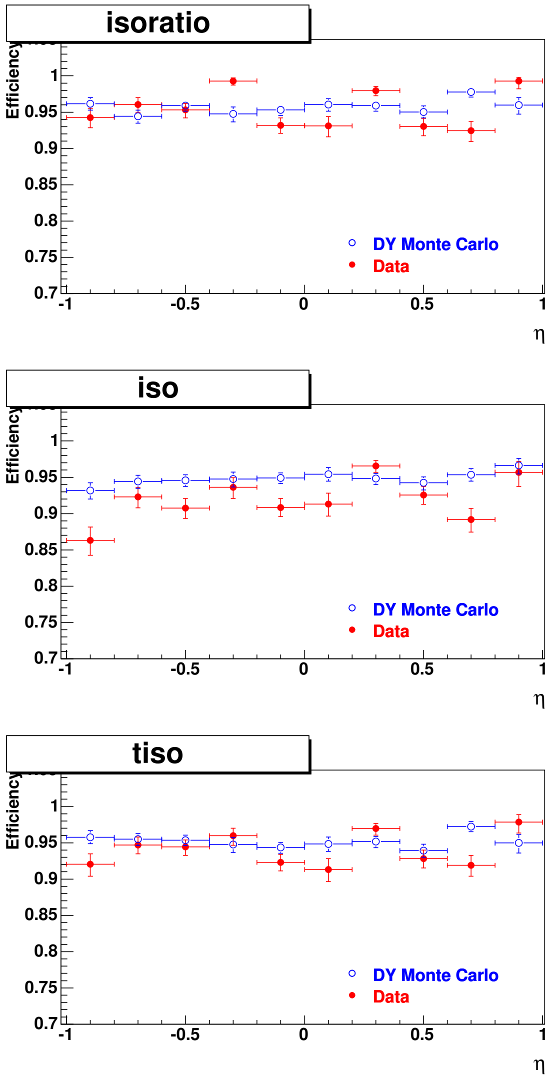

Figure 29: *The "ID" efficiencies of the isolation variables tested in the selection of the electron candidates, when all the cuts but the isolation itself are applied. All the efficiencies are plotted as a function of η of the second leg, in bins of 0.1, for 8* GeV *electron data (filled red dots) and DY Monte Carlo (empty blue dots).*

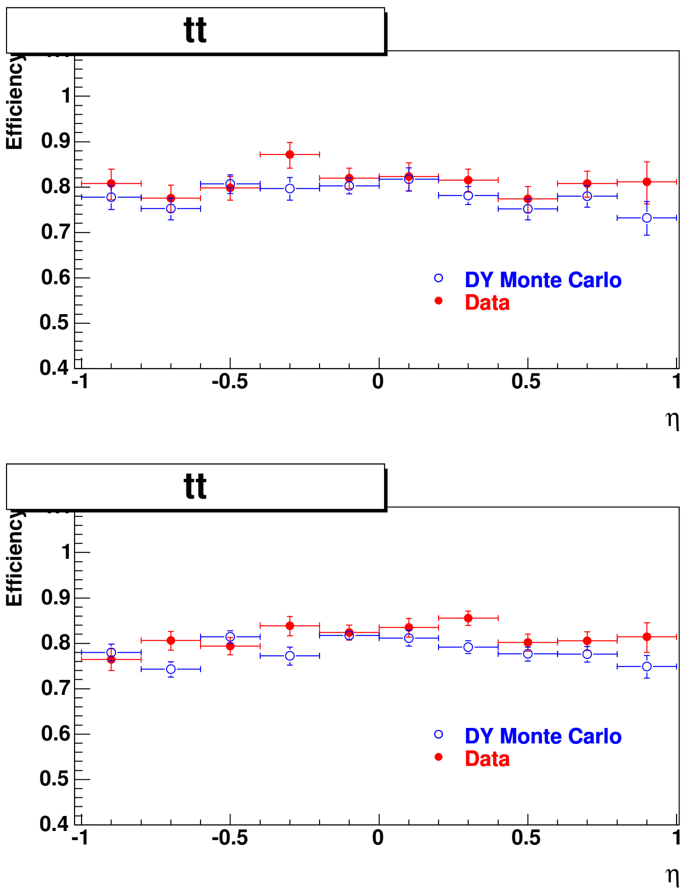

Figure 30: *The "N-1"(top) and ID(bottom) tight efficiencies, when all the cuts are applied. All the efficiencies are plotted as a function of η of the second leg, in bins of 0.1 for 8* GeV *electron data (filled red dots) and DY Monte Carlo (empty blue dots).*

A.3 Efficiencies as a function of ϕ

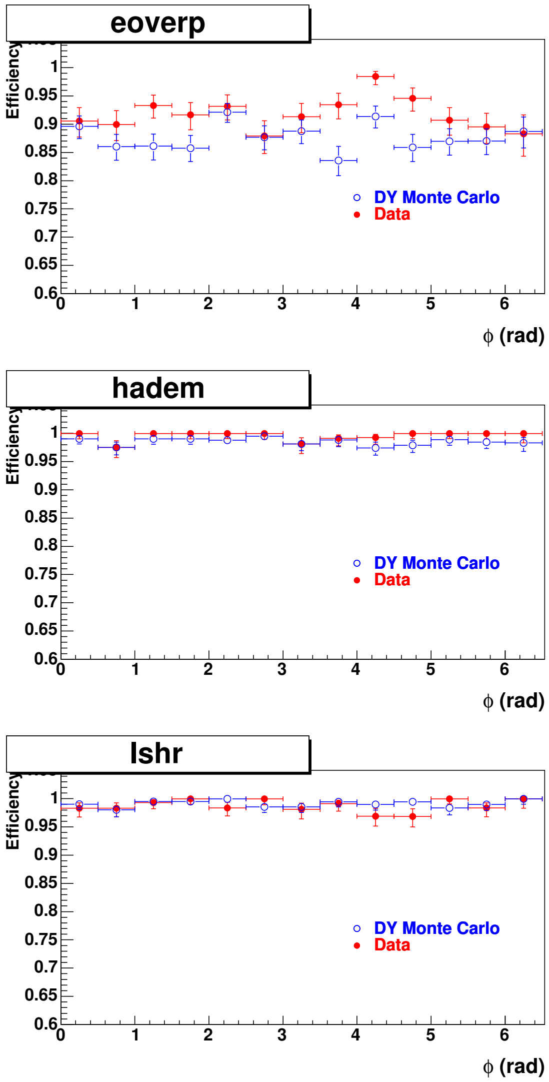

Figure 31: *The "N-1" efficiencies of the electron variables used in the selection of the electron candidates, when all the cuts but the one which is being tested are applied. All the efficiencies are plotted as a function of ϕ of the second leg, in bins of 0.5 radians, for 8* GeV *electron data (filled red dots) and DY Monte Carlo (empty blue dots).*

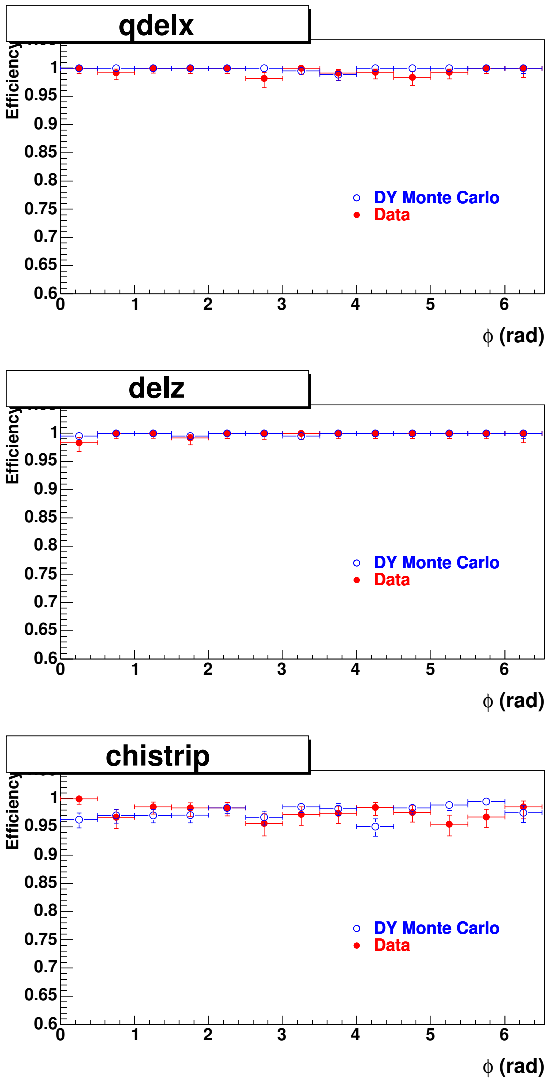

Figure 32: *The "N-1" efficiencies of the electron variables used in the selection of the electron candidates, when all the cuts but the one which is being tested are applied. All the efficiencies are plotted as a function of ϕ of the second leg, in bins of 0.5 radians, for 8* GeV *electron data (filled red dots) and DY Monte Carlo (empty blue dots).*

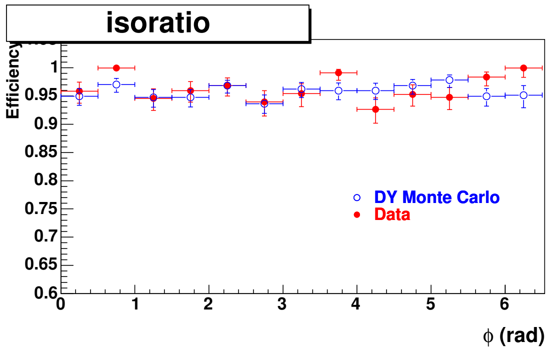

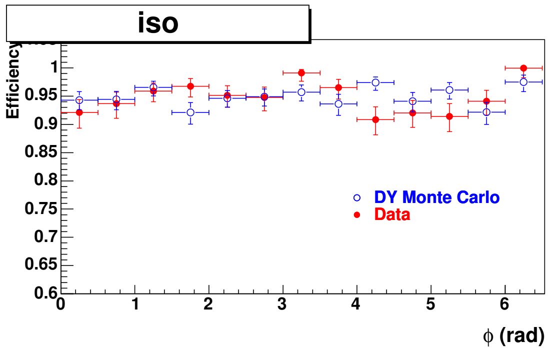

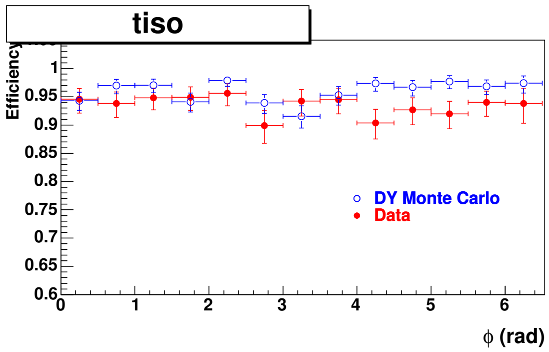

Figure 33: *The "N-1" efficiencies of the isolation variables tested in the selection of the electron candidates, when all the cuts but the isolation itself are applied. All the efficiencies are plotted as a function of ϕ of the second leg, in bins of 0.5 radians, for 8* GeV *electron data (filled red dots) and DY Monte Carlo (empty blue dots).*

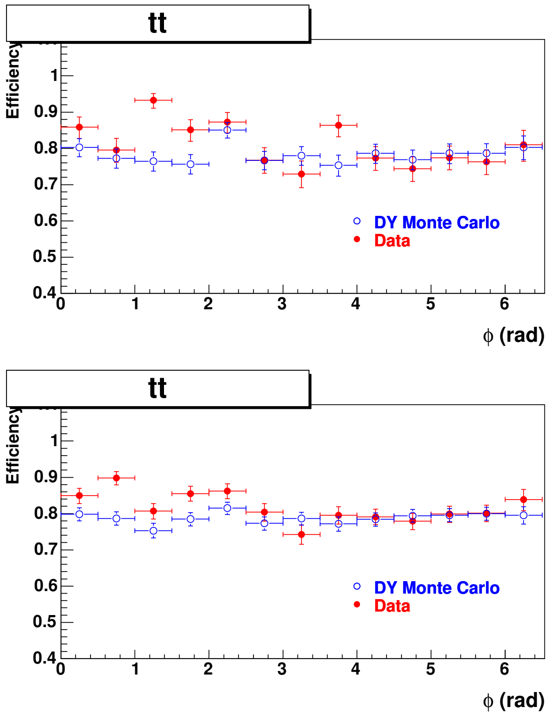

Figure 37: *The "N-1"(top) and ID(bottom) tight efficiencies, when all the cuts are applied. The efficiencies are plotted as a function of ϕ of the second leg, in bins of 0.5 radians, for 8* GeV *electron data (filled red dots) and DY Monte Carlo (empty blue dots).*

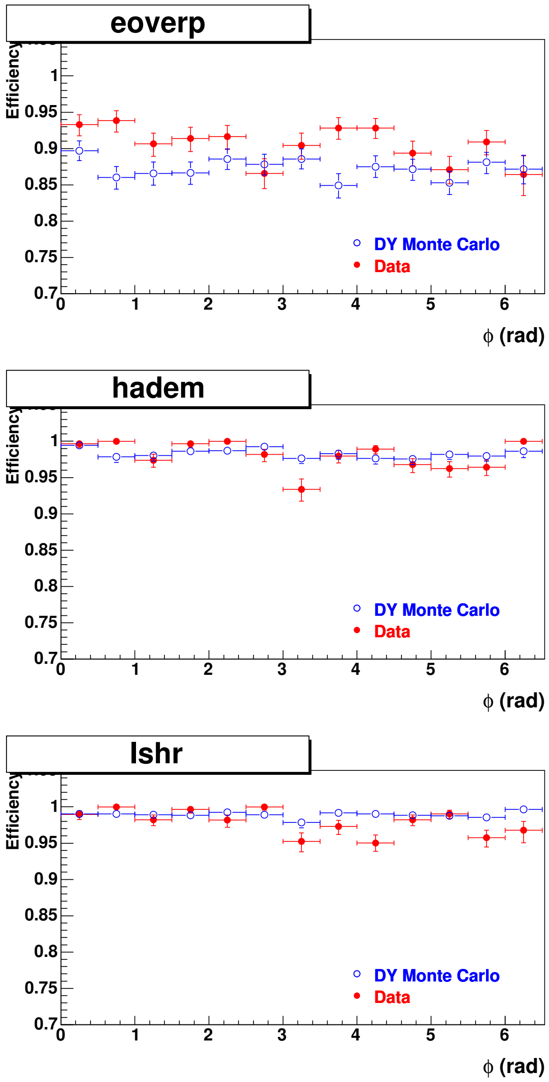

Figure 34: *The "ID" efficiencies of the electron variables used in the selection of the electron candidates, when all the cuts but the one which is being tested are applied. All the efficiencies are plotted as a function of ϕ of the second leg, in bins of 0.5 radians, for 8* GeV *electron data (filled red dots) and DY Monte Carlo (empty blue dots).*

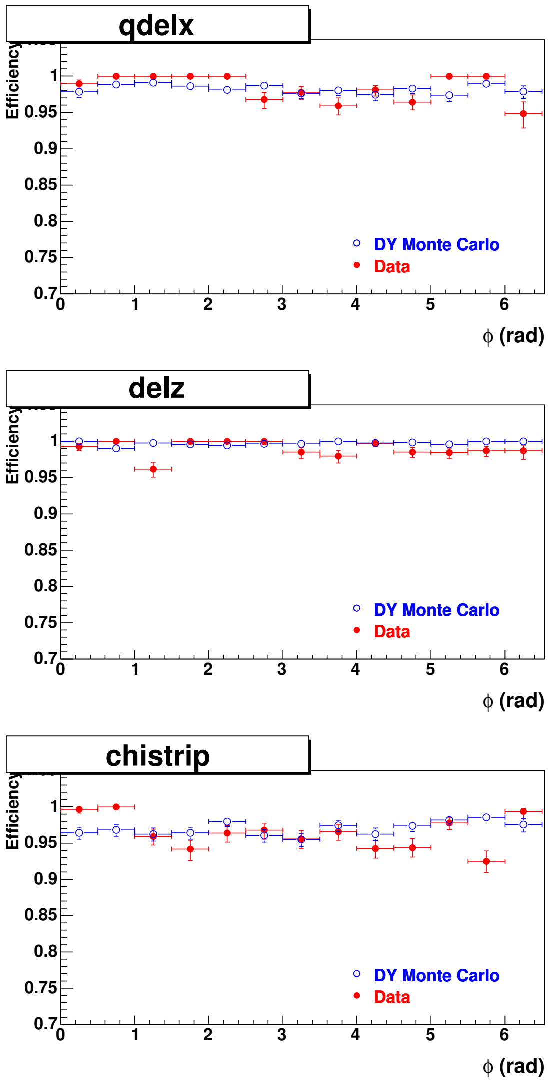

Figure 35: *The "ID" efficiencies of the electron variables used in the selection of the electron candidates, when all the cuts but the one which is being tested are applied. All the efficiencies are plotted as a function of ϕ of the second leg, in bins of 0.5 radians, for 8* GeV *electron data (filled red dots) and DY Monte Carlo (empty blue dots).*

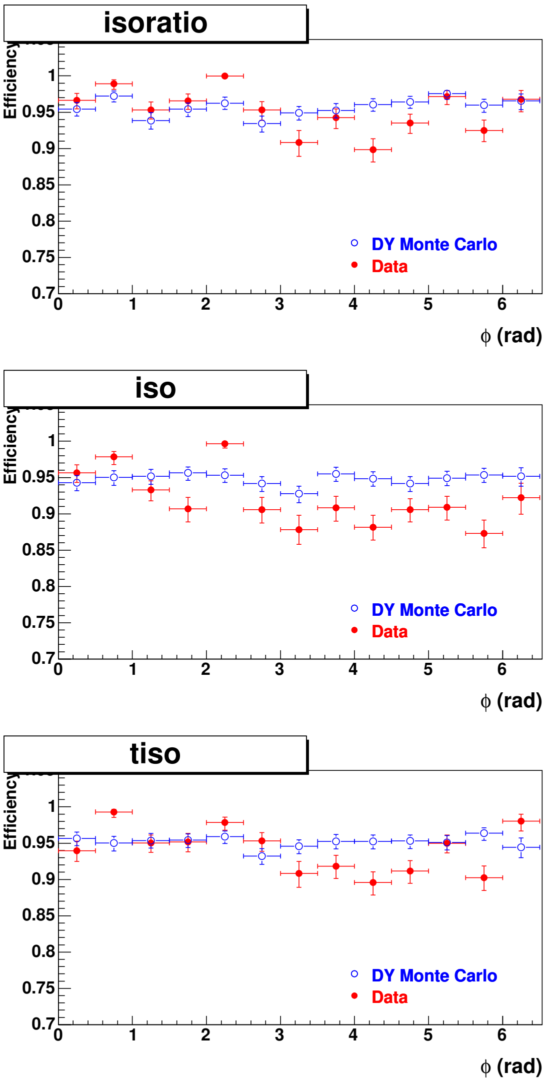

Figure 36: *The "ID" efficiencies of the isolation variables tested in the selection of the electron candidates, when all the cuts but the isolation itself are applied. All the efficiencies are plotted as a function of ϕ of the second leg, in bins of 0.5 radians, for 8* GeV *electron data (filled red dots) and DY Monte Carlo (empty blue dots).*

A.4 Efficiencies in the edil0d sample

The isolation variables are shown in Figure 38 and 39. The vertex studies are represented in Figure 40 and 41, while the invariant mass study is in Figure 42.

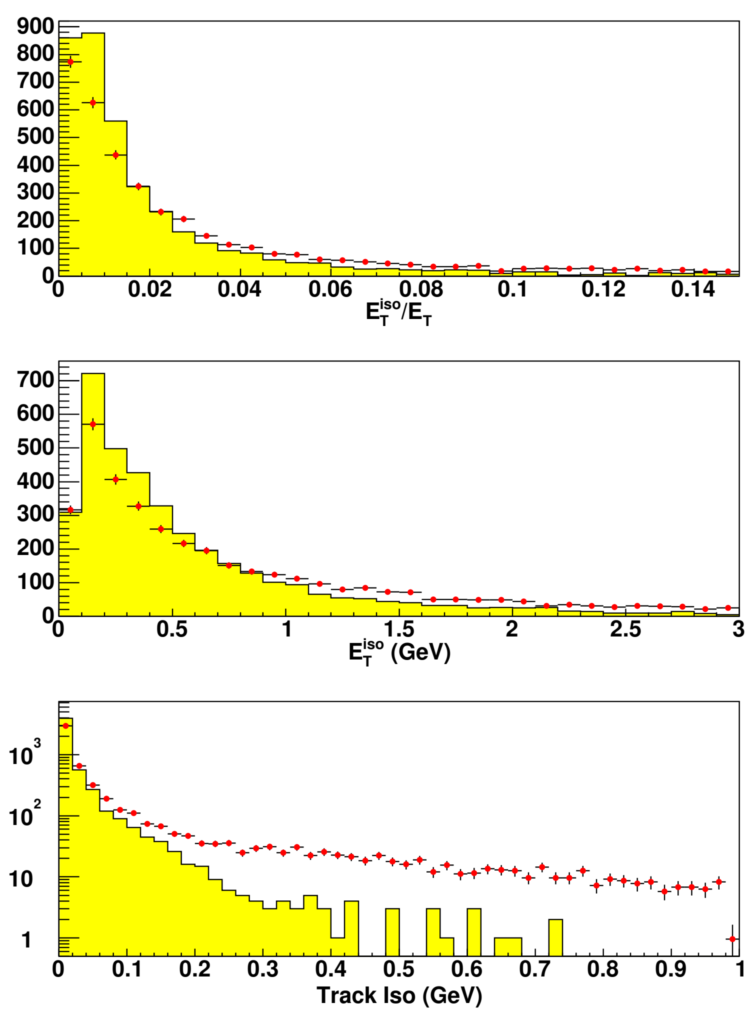

Figure 38: *The "N-1" distributions of the isolation variables:* E_T^{iso}/E_T*(top), track isolation (middle) and total isolation(bottom), for* DIELECTRON_CENTRAL_4 *data(dots) and DY Monte Carlo(solid histogram). The agreement is good for the calorimeter isolations. The shape of the track isolation in the data indicates the presence of the background.*

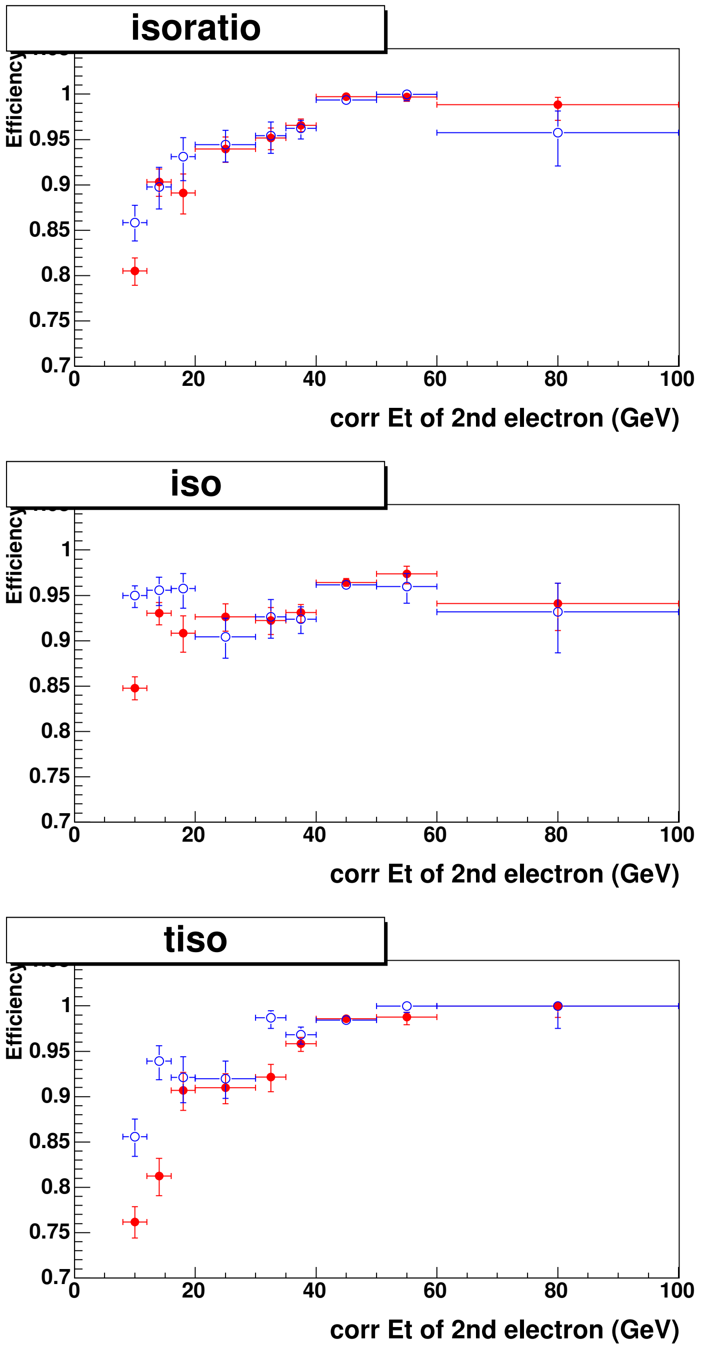

Figure 39: *The "N-1" efficiencies of the isolation variables tested in the selection of the electron candidates, when all the cuts but the isolation itself are applied. All the efficiencies are plotted as a function of the electromagnetic energy of the second leg, in bins of variable size as explained in the text, for* `DIELECTRON_CENTRAL_4` *data (filled red dots) and DY Monte Carlo (empty blue dots).*

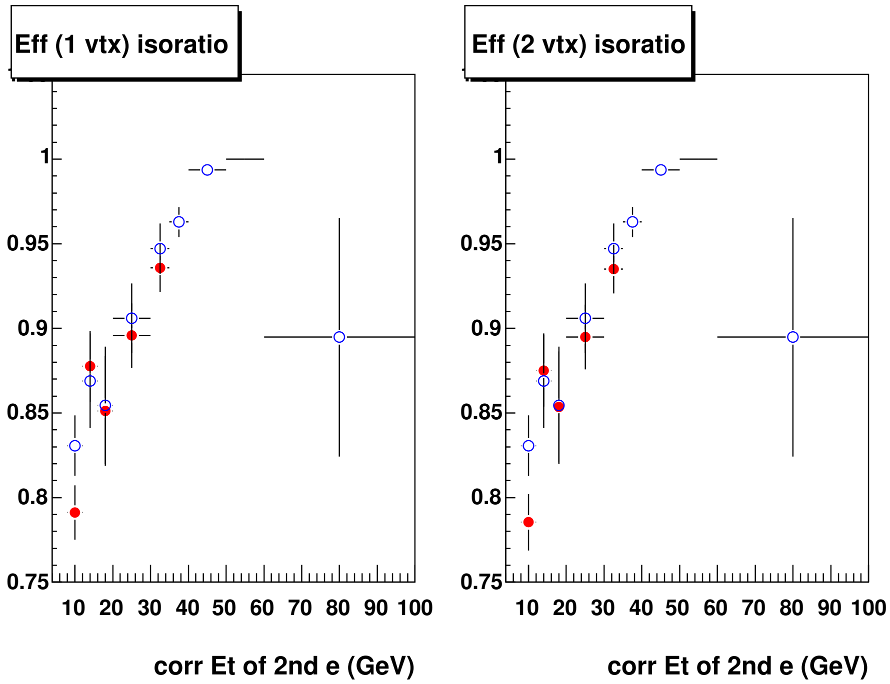

Figure 40: *The "N-1" efficiencies of the isolation variables when all the cuts but the isolation itself are applied, in the one-vertex (left) and two-vertices(right) bin. The efficiencies are plotted as a function of the electromagnetic energy of the second leg, in bins of variable size as explained in the text, for* DIELECTRON_CENTRAL_4 *data (filled red dots) and DY Monte Carlo (empty blue dots).*

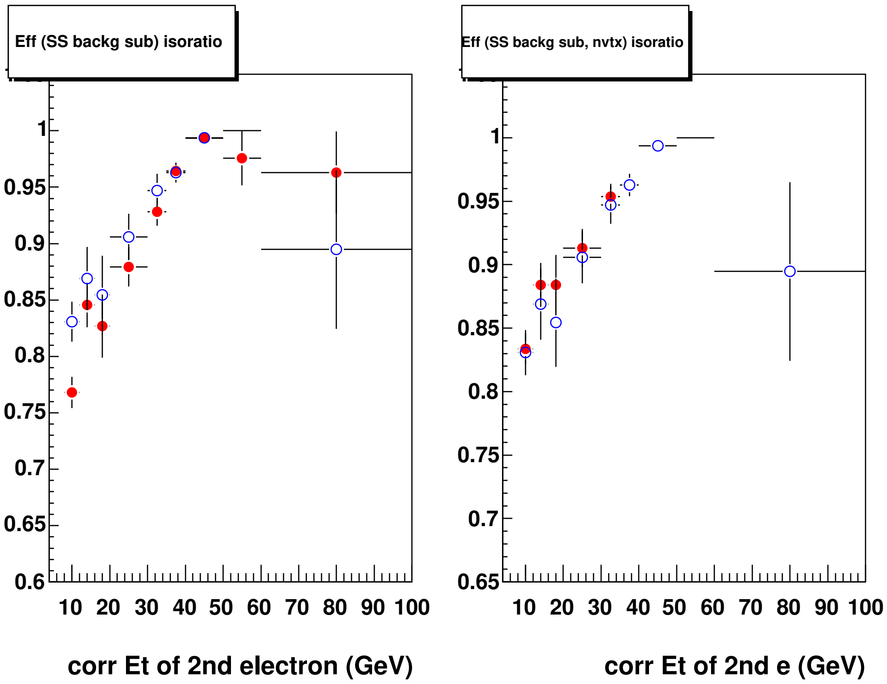

Figure 41: *The "N-1" efficiencies of the "isolation ratio" variable when all the cuts but the isolation itself are applied, with no correction(left) and when the correction for the number of vertices is applied(right). The plot on the left is the same as in Figure 9 and it is shown only for comparison. Both efficiencies are plotted as a function of the electromagnetic energy of the second leg, in bins of variable size as explained in the text, for* `DIELECTRON_CENTRAL_4` *data (filled red dots) and DY Monte Carlo (empty blue dots).*

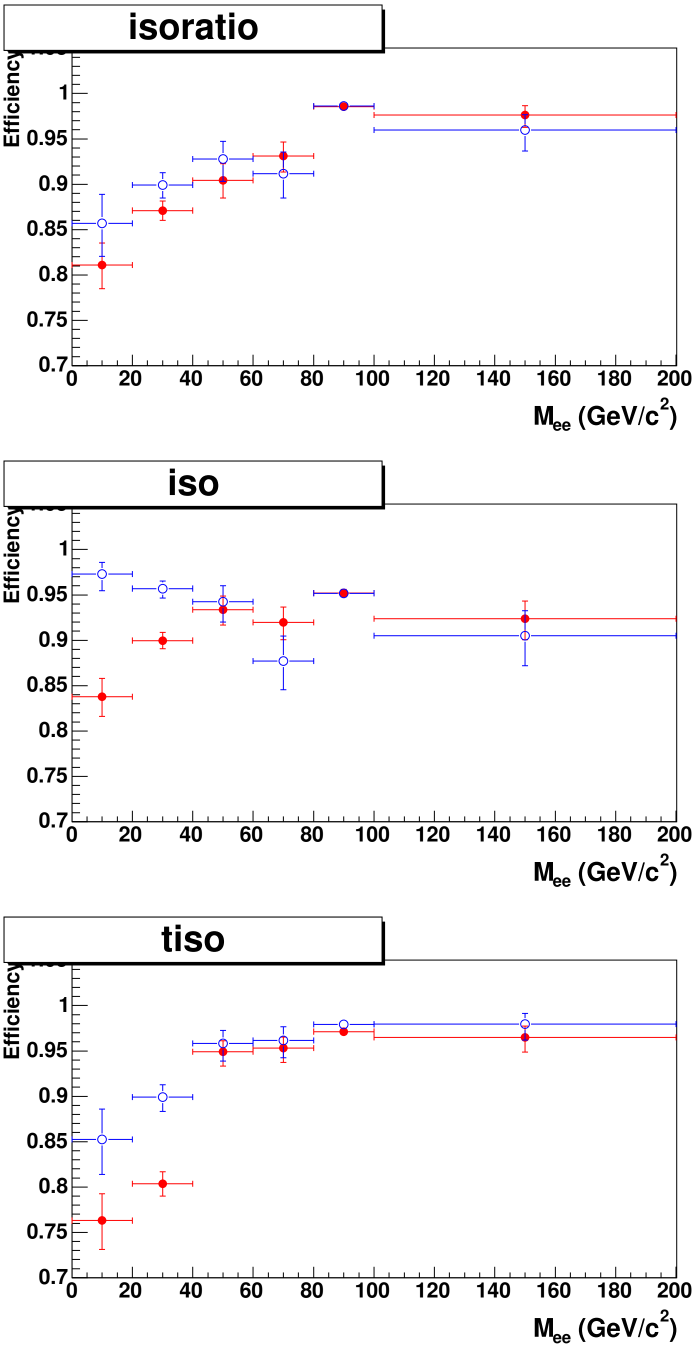

Figure 42: *The "N-1" efficiencies of the isolation variables when all the cuts but the isolation itself are applied, plotted as a function of the invariant mass of the two electrons, for* `DIELECTRON_CENTRAL_4` *data (filled red dots) and DY Monte Carlo (empty blue dots).*